Accepted Manuscript

Design, synthesis and biological evaluation of 7*H*-pyrrolo[2,3-*d*]pyrimidin-4-amine derivatives as selective Btk inhibitors with improved pharmacokinetic properties for the treatment of rheumatoid arthritis

Linhong He, Heyin Pei, Chufeng Zhang, Mingfeng Shao, Dan Li, Mingli Tang, Taijing Wang, Xiaoxin Chen, Mingli Xiang, Lijuan Chen

PII: S0223-5234(17)31110-8

DOI: 10.1016/j.ejmech.2017.12.079

Reference: EJMECH 10057

To appear in: *European Journal of Medicinal Chemistry*

Received Date: 24 August 2017

Revised Date: 22 December 2017

Accepted Date: 22 December 2017

Please cite this article as: L. He, H. Pei, C. Zhang, M. Shao, D. Li, M. Tang, T. Wang, X. Chen, M. Xiang, L. Chen, Design, synthesis and biological evaluation of 7*H*-pyrrolo[2,3-*d*]pyrimidin-4-amine derivatives as selective Btk inhibitors with improved pharmacokinetic properties for the treatment of rheumatoid arthritis, *European Journal of Medicinal Chemistry* (2018), doi: 10.1016/j.ejmech.2017.12.079.

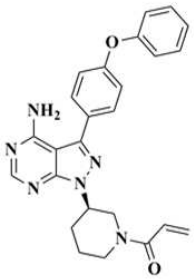

Ibrutinib
Btk IC_{50} = 0.81 nM
hERG IC_{50} = 0.97 μM
ClogP = 4.07
aqueous solubility < 0.01 mg/ml
F % in rats: 18-23%

structure-based design
PK studies and preliminary druglikeness evaluation

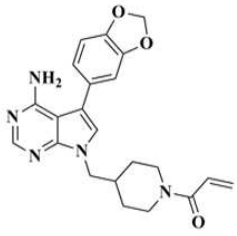

B16
Btk IC_{50} = 21.70 nM
hERG IC_{50} = 11.10 μM
ClogP = 2.53
aqueous solubility ≈ 0.1 mg/ml
F% in SD rat: 49.15%

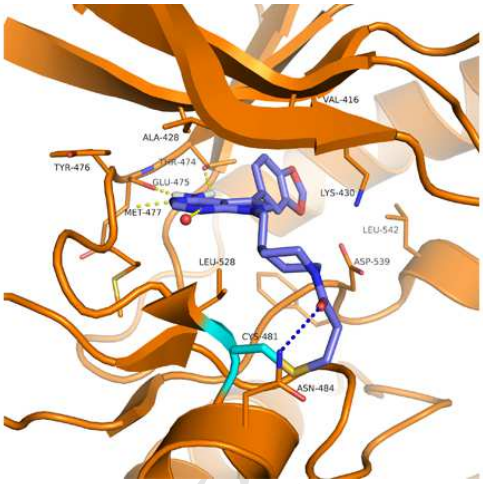

Design, synthesis and biological evaluation of 7*H*-pyrrolo[2,3-*d*]pyrimidin-4-amine derivatives as selective Btk inhibitors with improved pharmacokinetic properties for the treatment of rheumatoid arthritis

Linhong He[1,*], Heyin Pei[1,*], Chufeng Zhang[1,*], Mingfeng Shao[1], Dan Li[1], Mingli Tang[1], Taijing Wang[1], Xiaoxin Chen[2], Mingli Xiang[1], Lijuan Chen[1,#]

[1]State Key Laboratory of Biotherapy and Cancer Center, West China Hospital, Sichuan University and Collaborative Innovation Center. Chengdu, Sichuan 610041, PR China.

[2] Guangdong Zhongsheng Pharmaceutical Co., Ltd., Dongguan, Guangdong 523325, China.

[*]There authors contributed equally to this work.

[#]Corresponding Author

Lijiuan Chen

Tel: +86 28 85164063.

Fax: +86 28 85164060.

E-mail address: chenlijuan125@163.com (L-J. Chen)

Abstract: Bruton's tyrosine kinase (Btk) is a Tec family kinase with a well-defined role in the B cell receptor (BCR) and Fcγ receptor (FcR) signaling pathways, which makes it a uniquely attractive target for the treatment of autoimmune diseases, such as rheumatoid arthritis (RA). We reported a series of compounds bearing 7*H*-pyrrolo[2,3-*d*]pyrimidin-4-amine scaffold that potently inhibited Btk *in vitro*. Analysis of the structure-activity relationships (SAR) and drug-like profiles led to the discovery of the optimal compound **B16**. **B16** preferentially inhibited Btk (IC_{50} = 21.70 ± 0.82 nM) over closely related kinases with moderate selectivity. Cell-based tests also confirmed that **B16** significantly inhibited Btk Y223 *auto*-phosphorylation and PLCγ2 Y1217 phosphorylation. MTT revealed that **B16** displayed weak suppression against normal LO2, HEK293 and THP-1 cell lines with IC_{50} values over 30 μM. Moreover, **B16** showed very weak potential to block the hERG channel (IC_{50} = 11.10 μM) in comparison to ibrutinib (IC_{50} = 0.97 μM). Owing to its favorable physicochemical properties (ClogP = 2.53, aqueous solubility ≈ 0.1 mg/mL), pharmacokinetic profiles (F = 49.15%, $t_{1/2}$ = 7.02 h) and reasonable CYP450 profile, **B16** exhibited potent anti-arthritis activity and similar efficacy to ibrutinib in reducing paw thickness in CIA mice. In conclusion, **B16** is a potent, selective and durable inhibitor of Btk and has the potential to a safe and efficacious treatment for arthritis.

Key words: Btk, inhibitor, selectivity, bioavailability, aqueous solubility, rheumatoid arthritis

1. Introduction

Bruton tyrosine kinase (Btk) is a member of Tec family kinases including Tec, Itk, Txk and Bmx [1-4]. Btk is one of the most important drug target, since it broadly expresses in all hematopoietic cells except of plasma and T cells, and plays a critical role in B cell receptor (BCR) and Fcγ receptor (FcγR) signaling pathways, where it regulates the activation and proliferation of B cells [5-6]. Upon activation by upstream kinases (such as Lyn and Syk), Btk subsequently phosphorylates and activates phospholipase-Cγ (PLCγ), leading to calcium ion transportation and activation of NF-κB and MAP kinase pathways [1-6]. Thus, Btk is involved in pro-inflammatory signals and regulates the expression of pro-inflammatory cytokines, chemokines and cell adhesion molecules. Taken together, Btk's role in these pathways makes it a uniquely attractive target for the treatment of B cell related diseases, such as the autoimmune disorder rheumatoid arthritis (RA) [1-6].

RA is an autoimmune disease that involves systemic dysregulation of T and B lymphocytes with immune responses against self-antigens, and ultimately resulting in circulating autoantibodies, synovial inflammation, pannus formation, and cartilage and bone destruction in affected joints [7-8]. B cell function and autoantibody production have been proven to promote the progression of RA [1,7-8]. The treatment of RA with anti-CD20 antibody rituximab to deplete mature B cells in clinical studies, clearly demonstrates that therapies directly or indirectly targeting B cells have the potential to attenuate disease progression of RA [9-10]. Pharmacological and genetic studies in animal models also verify Btk inhibitors can be efficacious against RA [3-6]. Moreover, RANK signaling is Btk dependent and controls osteoclastogenesis from monocytic precursors [5,6]. Therefore, Btk has been identified as a potent target for the treatment of RA. During recent years, more and more Btk inhibitors have been developed and demonstrated efficacies in preclinical animal models for RA (ibrutinib, RN486, CGI1746 and so on) or entered into clinical trials for RA (CC-292 and HM71224) (**Figure 1**) [9-11].

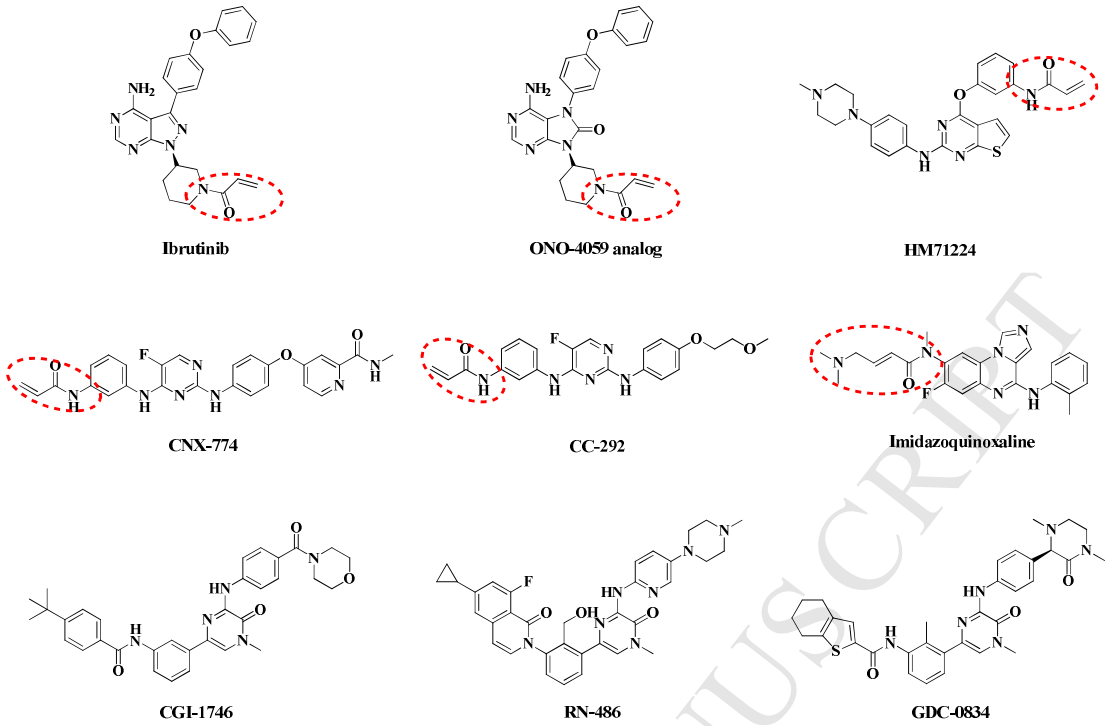

Figure 1. Btk inhibitors in development for RA

Until now, the most successful Btk inhibitor is ibrutinib, which has been clinically used for the treatment of mantle cell lymphoma (MCL), chronic lymphatic lymphoma (CLL), and waldenström's macroglobulinemia (WM) [12-13]. Owing to its excellent inhibition to Btk, ibrutinib not only efficiently reverses arthritic inflammation in a therapeutic collagen induced arthritis (CIA) models, but also prevents clinical arthritis in collagen antibody-induced arthritis (CAIA) models, indicating its potential use for the treatment of RA [14-15]. However, ibrutinib can also strongly inhibit numerous kinases with structural homology, such as EGFR, JAK3, and ErbB2 [12,14,16], which can lead to significant toxicities, including bleeding, myelosuppression, diarrhea, atrial fibrillation (AF) and renal impairment [16-19]. Potent inhibition of EGFR by ibrutinib may explain the observed diarrhea, which has been observed in clinical practices with EGFR inhibitors [19]. The moderate inhibition against hERG current (IC_{50} = 0.97 μM) by ibrutinib is considered as a low-potency blocker and closely associated with AF [18,20]. RA, quite different from hematological malignancies, is a non-life-threatening disease that calls for safe

therapies with unexpected off-target toxicities [13]. This has encouraged the development of more selective Btk inhibitors, including GDC-0834 and RN-486, but GDC-0834 was suspended in phase I because of its poor pharmacokinetics (PK) properties [13,21,22]. Hence, developing highly selective Btk inhibitors with favorable PK properties will be more suitable and efficacious to fulfill the treatment need for RA disease [13,21,22].

Encouraged by the excellent anti-arthritis activity of ibrutinib, we decided to optimize the structure of ibrutinib in an attempt to improve its kinase selectivity, toxicity and PK profiles. Given that the scaffolds of Btk inhibitors are major representative structures [23,33], and replacing the central core of ibrutinib with 6-amino-7*H*-purin-8(9*H*)-one (ONO-4059) maintains the potency of inhibiting Btk [19], we selected 7*H*-pyrrolo[2,3-*d*]pyrimidin-4-amine as the new scaffold to replace the pharmacophore of ibrutinib by employing the theory of bioisostere. As illustrated in **Figure 2**, similar to ibrutinib, 7*H*-pyrrolo[2,3-*d*]pyrimidin-4-amine scaffold can also occupy the ATP binding pocket and make several important hydrogen bond interactions with respective Thr474, Glu475 and Met477 in the hinge. 4-Piperidinylmethyl was selected as a linker to connect the scaffold and electrophilic warheads, which allowed acrylamide to form a covalent bond with the conserved Cys481 residue in Btk domain. As expected, the phenoxyphenyl group of **B1** was overlaid with the same fragment of ibrutinib, which completely entered the hydrophobic pocket and formed a face-to-edge π-stacking interaction with Phe540. In our effort to improve the ClogP, aqueous solubility, as well as PK profiles, structural modifications on C3-position of pyrryl was firstly performed. In the further research of exploring the structure-activity relationships (SAR) of this series derivatives and hunting for more potent Btk inhibitors, structural modifications were also conducted on linker, scaffold and electrophilic warhead region. Herein, we report the synthesis and pharmacological evaluation of these novel compounds as potent Btk inhibitors, of which the representative compound **B16** exhibits excellent kinase selectivity to Btk, low toxicity, favorable PK properties and good efficacy for the treatment of RA

though oral administration.

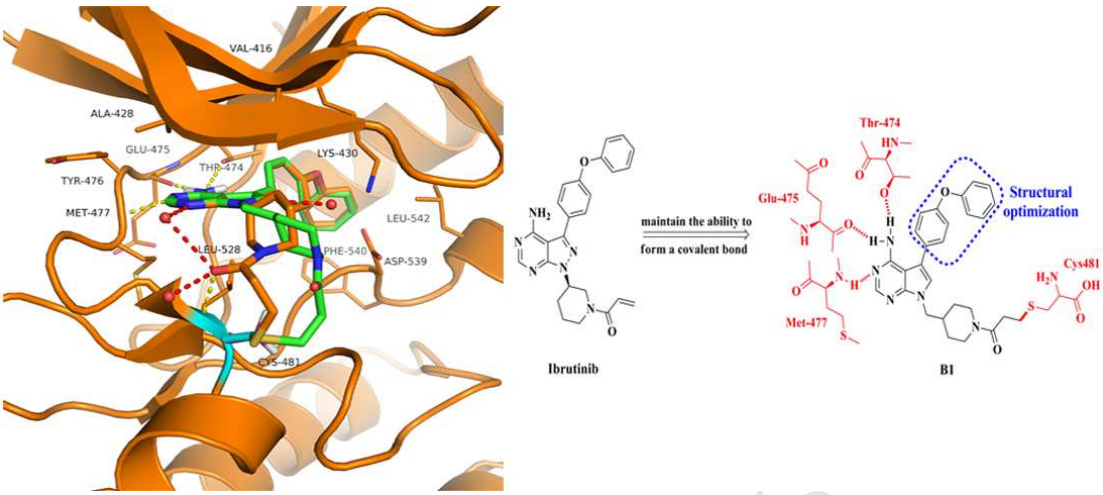

Figure 2. Design of the 7*H*-pyrrolo[2,3-*d*]pyrimidin-4-amines as Btk inhibitors. A covalent docking model: similar to ibrutinib, compound **B1** also can form a covalent bind with the conserved cys481 residue in Btk domain (ibrutinib: orange; **B1**: green).

2. Compounds synthesis

The synthesis route of compounds **B1-B24** is described in **Scheme 1**. By reference to the preparation of ibrutinib, the starting material **1-1** was directly coupled with **4** by Mitsunobu reaction in an extremely low yield. In order to improve the chemical reactivity of **1-1**, it was treated with methanesulfonyl chloride in an ice bath and subsequently with lithium bromide under reflux overnight, giving the important intermediate **3** that allowed completely reaction with **4** to offer **5** in a good yield. **5** was reacted with ammonia (con.) in an autoclave to give **6**, then coupled with a variety of boronic acid derivatives via Suzuki-Miyaura cross-coupling procedure to provide **7**. Intermediate **8** was obtained by removing the Boc group from **7** in an acid condition. Finally, the classical electrophilic warhead acryloyl group was introduced to **8** giving final products **B1-B24**.

Scheme 1. Preparation of compounds **B1**-**B24**.

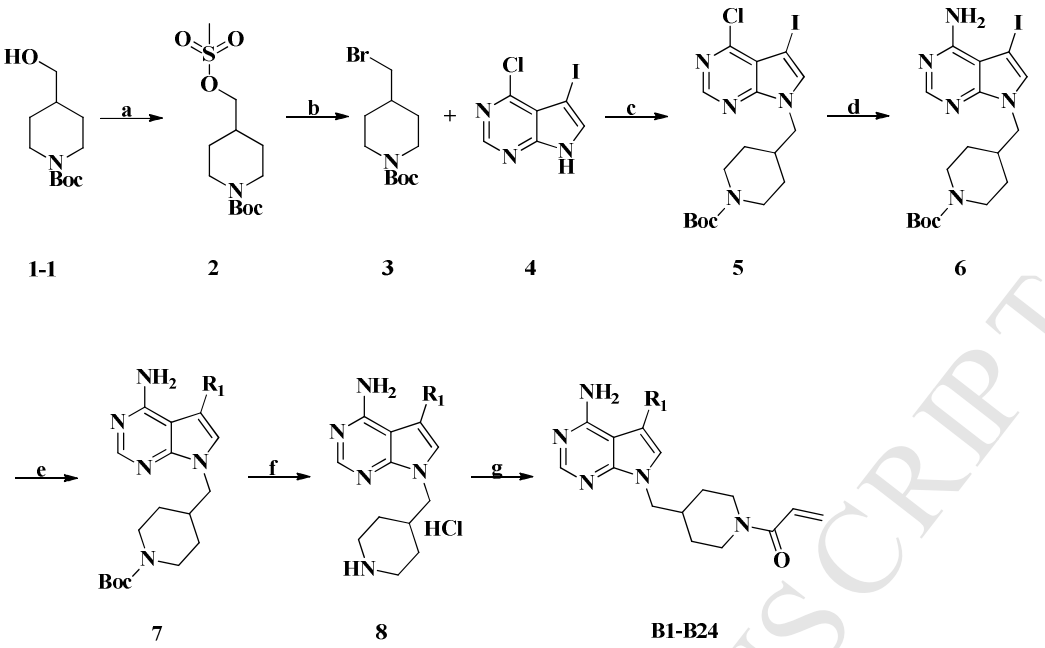

Reactions and conditions: (**a**) MsCl, Et_3N, DCM, 0 ºC, 2 h; (**b**) LiBr, ACE, reflux, overnight; (**c**) K_2CO_3, DMF, 80 ºC, 3-4 h; (**d**) NH_4OH, 1,4-dioxane, 98 ºC, overnight; (**e**) boronic acid (R_1), K_2CO_3, $PdCl_2$(dppf), 1,4-dioxane/H_2O, 98 ºC, 3-4 h; (**f**) 1,4-dioxane, HCl in 1,4-dioxane, 50 ºC, overnight; (**g**) acryloyl chloride, DIEA, dry DMF, r.t., 2 h.

To search the SAR of linker connecting 7*H*-pyrrolo[2,3-*d*]pyrimidin-4-amine and electrophilic warheads, we synthesized another three kinds of analogues containing favorable side chains of 4-phenoxyphenyl or benzo[*d*][1,3]dioxol-5-yl on the scaffold. Target compounds **B25-B26** were prepared according to the same procedures in **Scheme 1** from the starting material of (*R*)-tert-butyl-3-(hydroxymethyl)piperidine-1-carboxylate (**1-2**), while **B27-B28** and **B29-B30** were obtained from (*S*)-tert-butyl-3-(hydroxymethyl)piperidine-1-carboxylate (**1-3**) and tert-butyl-4-(2-hydroxyethyl) piperidine-1-carboxylate (**1-4**), respectively.

Scheme 2. Preparation of compounds **B25-B30.**

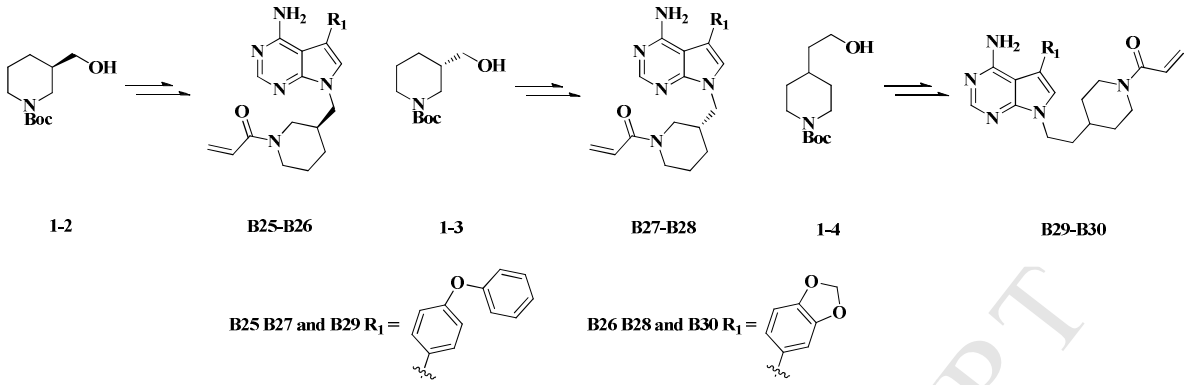

On the basis of the potent compounds **B1** and **B16**, analogues **B31**-**B34** also had been synthesized to evaluate the functions of electrophilic warheads, and their synthesis routes were shown in **Scheme 3**. Intermediate **8-1** was treated with 2-chloroethanesulfonyl chloride in anhydrous dichloromethane giving **B31**, while **B33** was obtained in the same way from **8-16**. Another two compounds **B32** and **B34** were provided by coupling (*E*)-4-(dimethylamino)but-2-enoic acid with respective amides in low yields (< 35%).

Scheme 3. Preparation of compounds **B31**-**B34**

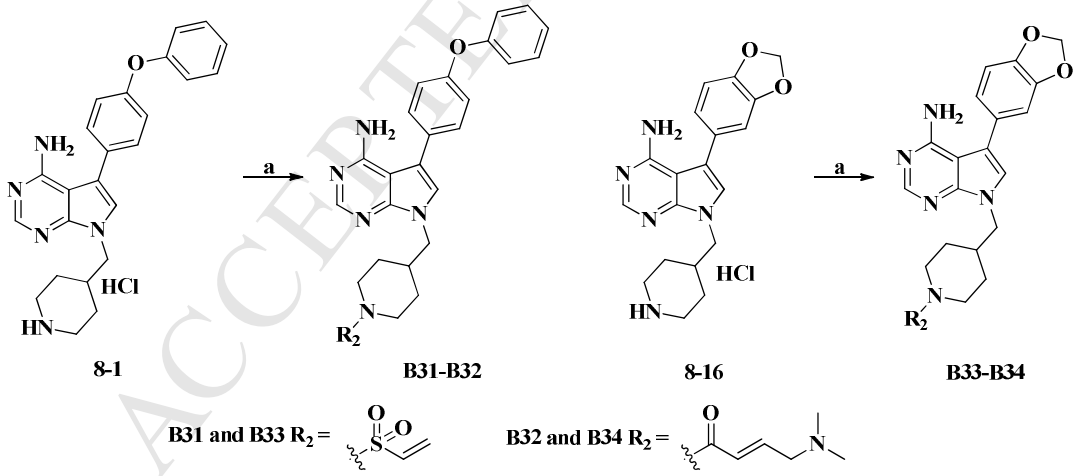

Reactions and conditions: (**a**) **B31** and **B33**, 2-chloroethanesulfonyl chloride, DIEA, dry DCM, r.t., 1 h; **B32** and **B34**, (*E*)-4-(dimethylamino)but-2-enoic acid hydrochloride, DIEA, PyBOP, DCM, r.t., overnight.

Then we focused on the structural modifications on the scaffold region. As

described in **Scheme 4**, compounds bearing 1*H*-pyrazolo[3,4-*d*]pyrimidin-4-amine, the scaffold of ibrutinib, were also prepared. Commercially available material 1*H*-pyrazolo[3,4-*d*]pyrimidin-4-amine (**9**) was reacted with n-iodosuccinimide (NIS) to offer **10**, and the following reactions were similar as in **Scheme 1**. Eventually, we got new compounds **B35**-**B38**.

Scheme 4. Preparation of compounds **B35**-**B38**

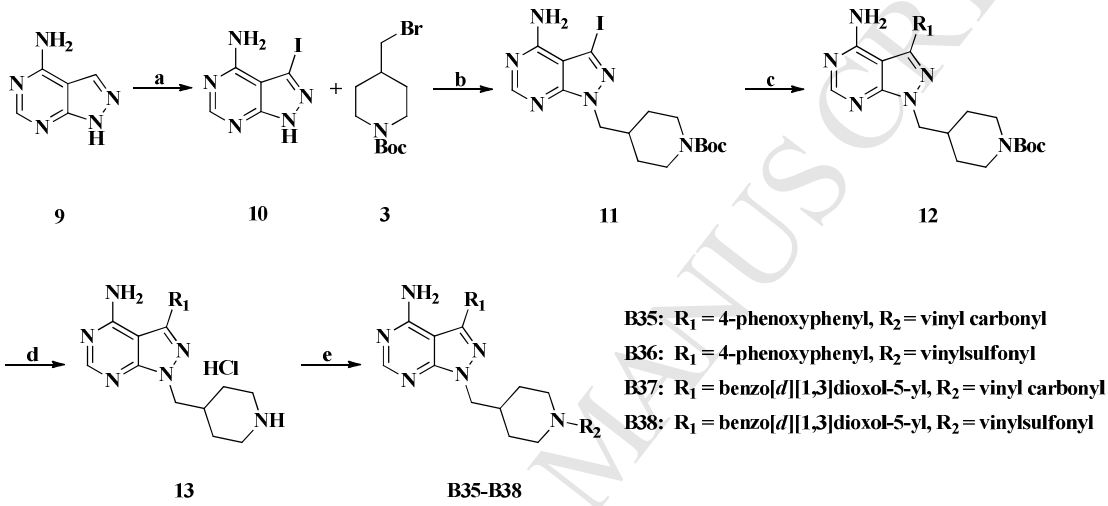

Reactions and conditions: (**a**) NIS, DMF, r.t., 2 h; (**b**) K_2CO_3, DMF, 80 ºC, 3-4 h; (**c**) K_2CO_3, $PdCl_2$(dppf), 1,4-dioxane/H_2O, 98 ºC, 3-4 h; (**d**) 1,4-dioxane, HCl in 1,4-dioxane, 50 ºC, overnight; (**e**) **B35** and **B37**, acryloyl chloride, DIEA, dry DMF, r.t., 2 h; **B36** and **B38**, 2-chloroethanesulfonyl chloride, DIEA, dry DCM, r.t., 1 h.

3. Result and discussion

3.1 *In vitro* potency

All the synthesized compounds were assessed the inhibitory activities against Btk at the concentrations of 1 μM and 0.1 μM, and the results were summarized in **Table 1**. As expected, compound **B1** with 4-phenoxyphenyl substitution, structurally similar to ibrutinib, displayed a strong Btk inhibition potency. The potency of **B1** slightly decreased by contrast to ibrutinib. (**Figure 2**). Compounds with 4-(benzyloxy)phenyl (**B2**) and 4-(3,4-difluorobenzyloxy)phenyl (**B24**) substitutions decreased the potencies of inhibiting Btk, which may due to their large substituent

groups interfered in forming π-stacking interaction. The 4-(pyridin-2-yloxy)phenyl (**B3**) substitution also could not maintain excellent potency that probably attributed to its lower hydrophobicity than **B1**. The 4-fluorophenyl analogue (**B7**) was more potent than 3-chlorophenyl (**B6**) substitutions. Nevertheless, the potencies decreased as the volume of substituent groups increased (**B8** and **B9**). Similar trend was observed on 4-hydroxyphenyl compound (**B12**) and its derivatives (**B13**, **B14** and **B15**). Surprisingly, compound **B16** substituted with benzo[*d*][1,3]dioxol-5-yl exhibited good inhibition to Btk, but other fused heterocyclics (**B18**, **B21** and **B22**) slightly decreased the efficacies of inhibiting Btk. Compounds with polar groups on phenyl, such as **B4**, **B11** and **B19**, dramatically lost in activities might be attributed to the missing π-stacking and hydrophobic interactions in the hydrophobic pocket. In brief, compounds **B1** and **B16** were worth further structural optimizations.

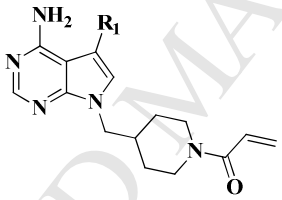

Table 1 The structure of **B1**-**B24** and their activities in enzymatic assay [a]

Comp.	R_1	Btk Mean_inh%		Comp.	R_1	Btk Mean_inh%	
		1 μM	0.1 μM			1 μM	0.1 μM
Ibruti -nib	-	99.6 ± 0.1	99.3 ± 0.5	**B13**	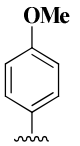	89.7 ± 0.2	39.5 ± 0.2
B1	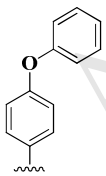	97.6 ± 0.0	94.1 ± 0.3	**B14**	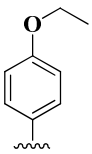	87.4 ± 0.21	35.8 ± 0.52
B2	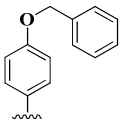	91.0 ± 1.4	54.0 ± 2.6	**B15**	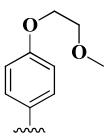	84.3 ± 0.5	32.6 ± 0.8

B3	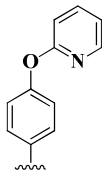	90.0 ± 0.1	45.3 ± 0.5	**B16**	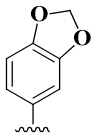	98.3 ± 1.1	82.4 ± 0.2
B4	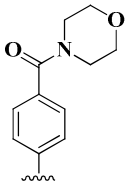	8.3 ± 0.4	6.5 ± 4.4	**B17**	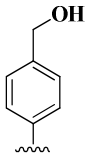	73.5 ± 20.5	0.6 ± 4.4
B5	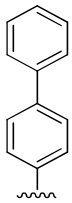	43.1 ± 4.6	12.5 ± 6.5	**B18**	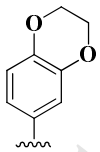	88.6 ± 1.5	31.7 ± 1.1
B6	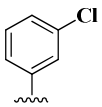	73.3 ± 0.4	6.5 ± 4.4	**B19**	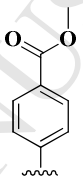	34.9 ± 3.8	12.4 ± 1.6
B7	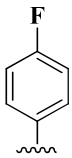	92.8 ± 0.9	50.3 ± 1.5	**B20**	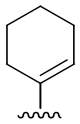	73.3 ± 0.9	18.4 ± 5.4
B8	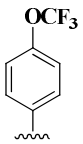	52.8 ± 0.4	9.2 ± 4.1	**B21**	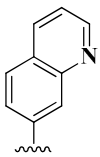	62.4 ± 4.0	14.9 ± 2.6
B9	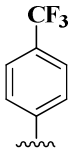	73.6 ± 1.4	16.0 ± 0.5	**B22**	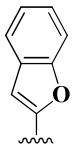	78.2 ± 1.5	17.0 ± 2.7
B10	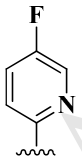	94.2 ± 0.5	47.4 ± 6.0	**B23**	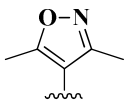	16.6 ± 1.6	4.7 ± 4.7
B11	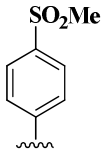	34.0 ± 1.9	14.7 ± 2.0	**B24**	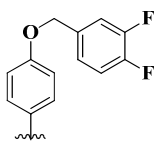	52.7 ± 5.7	10.6 ± 1.2
B12	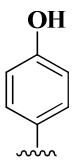	94.9 ± 0.0	48.5 ± 1.1				

[a] Enzymatic assay is performed in the presence of ATP concentration at K_m 90 μM. Mean_inh% represents Mean ± SD from at least two independent experiments.

In order to investigate the SAR of linker, we further synthesized 3-piperidinylmethyl analogues, including *R*-enantiomers (**B25** and **B26**) and *S*-enantiomers (**B27 and B28**). Unfortunately, neither of them displayed better potencies of inhibiting Btk than the corresponding 4-piperidinylmethyl analogues except **B27** (**Table 2**). Unlike the *R* enantiomer of ibrutinib, **B27** is *S* enantiomer and slightly decreased the activity in contrast to ibrutinib. Another two 4-piperidinoethyl derivatives, **B29** and **B30**, were also less potent than the corresponding 4-piperidinylmethyl ones.

Common electrophilic warheads (*E*)-2-(4-(dimethylamino)but-2-vinyl and vinylsulfonyl were respectively introduced to the bottom piperidyl in an attempt to increase the inhibitory activity to Btk. In comparison to vinyl carbonyl, vinylsulfonyl substitution (**B31** and **B33**) did some improvement in activity, implying that sulfuryl can form a stronger covalent bond with cysteine than vinyl carbonyl. Unfortunately, the modification on vinyl carbonyl (**B32** and **B34**) resulted in different degrees of loss in activities, and **B34** even totally lost the potency of inhibiting Btk, of which *N*,*N*-dimethyl substitution might interfere vinyl carbonyl to form a covalent bond with cysteine. It could be simply summarized that most compounds with benzo[*d*][1,3]dioxol-5-yl substitution on C3-position of pyrryl exhibited less potentials of inhibiting Btk than the 4-phenoxyphenyl analogues.

Table 2. *In vitro* potencies of selected compounds [a,b,c]

Comp.	Btk IC_{50}/nM [a]	ClogP [b]	aqueous solubility (mg/mL) [c]	Comp.	Btk IC_{50}/nM [a]	ClogP [b]	aqueous solubility (mg/mL) [c]
ibrutinib	0.81 ± 0.11	4.07	< 0.01	**B28**	500.21 ± 1.01	2.53	≈ 0.1
B1	6.09 ± 1.45	4.66	< 0.01	**B29**	36.83 ± 0.93	5.19	< 0.01
B2	77.04 ± 0.73	4.25	< 0.01	**B30**	597.81 ± 1.24	3.06	< 0.1

B16	21.70 ± 0.82	2.53	≈ 0.1	**B31**	4.24 ± 2.05	4.70	< 0.01
B25	7.34 ± 0.92	4.66	< 0.01	**B32**	25.64 ± 1.03	4.98	< 0.01
B26	83.55 ± 0.91	2.53	≈ 0.1	**B33**	1.32 ± 1.20	2.57	≈ 0.1
B27	1.71 ± 1.54	4.66	< 0.01	**B34**	2369.28 ± 1.01	2.84	< 0.1

[a] IC_{50} values of Btk are an average of at least three independent dose-response curves at K_m ATP (5 nM Btk and 90 μM ATP), mean ± SD. [b] ClogP values are calculated by ChemBioDraw software Ultra 12.0. [c] The solubility was measured by a method as follows: 1.0 mg of the appropriated compound dissolved in 1.0 mL of water at ambient temperature, continuous another 1.0 mL of water was added until the compound was completely dissolved.

In order to explain the different enzymatic potencies of those compounds respectively substituted with benzo[*d*][1,3]dioxol-5-yl and 4-phenoxyphenyl on the C3-position of pyrryl and find out their interactions, compounds **B1** and **B16** were selected to dock into Btk protein domain using the program Covalent Dock Clound. As illustrated in **Figure 3A**, similar to **B1** (**Figure 2**), **B16** maintained the potential to form three key hydrogen bond interactions with respective Thr474, Glu475 and Met477 in the hinge, and a covalent bond with Cys481. Although the carbony on **B16** was clearly observed to form another H-bond with Asn484, this interaction was lower than the π-stacking interaction with Phe540 in comparison to ibrutinib. The analysis of hydrophobic interactions between Btk protein and selected compounds explained that the slight potency decrease of **B16** was not only attributed to its weaker hydrophobicity of benzo[*d*][1,3]dioxol-5-yl than phenoxyphenyl group on **B1** or ibrutinib, but also not completely filled of the hydrophobic pocket.

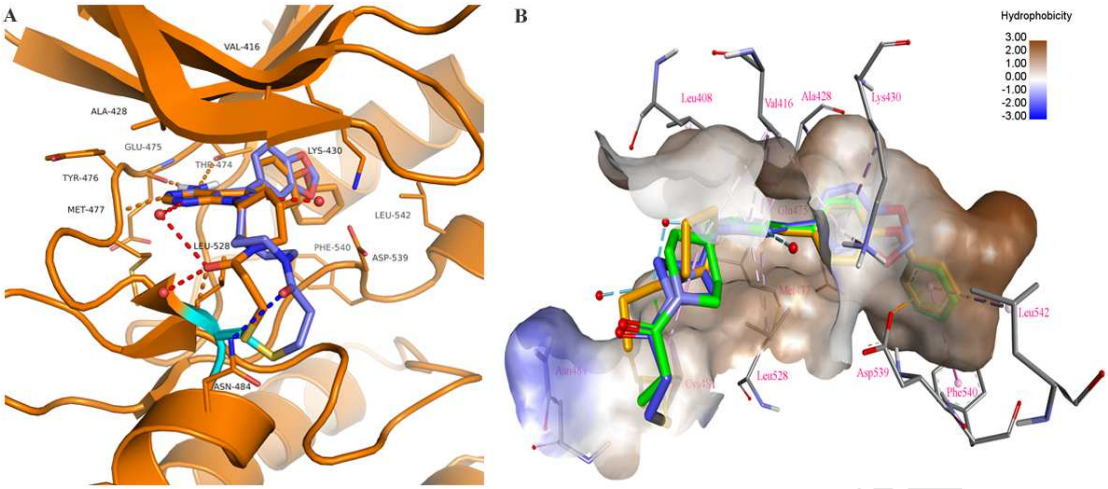

Figure 3. Selected compounds docked into Btk kinase domain. (**A**): Analysis of compound **B16** and ibrutinib binding into Btk kinase domain (**B16**: purple; ibrutinib: orange). (**B**): The analysis of hydrophobic interaction between Btk protein and selected compounds **B1**, **B16** and ibrutinib (**B1**: green; **B16**: purple; ibrutinib: orange).

Taken the docking results together, the scaffold of ibrutinib was found to form one more hydrogen bond interaction with water molecules than the pharmacophore of **B1** and **B16**. On the basis of this finding, we had synthesized compounds **B35-B38** bearing the scaffold of ibrutinib. As expected, compounds **B35** and **B36** slightly increased the potencies of inactivating Btk in comparison to the corresponding compounds **B1** and **B31**. However, on the contrary, benzo[*d*][1,3]dioxol-5-yl analogues, **B37** and **B38**, were both weaker to inhibit Btk than **B16** and **B33**, respectively.

Table 3. *In vitro* potencies of selected compounds [a,b,c]

Comp.	Btk IC_{50}/nM [a]	ClogP [b]	aqueous solubility (mg/mL) [c]	Comp.	Btk IC_{50}/nM [a]	ClogP [b]	aqueous solubility (mg/mL) [c]
ibrutinib	0.80 ± 0.07	4.07	< 0.01	**B37**	70.70 ± 1.14	1.91	≈ 0.1
B35	2.46 ± 1.57	4.08	< 0.01	**B38**	3.22 ± 1.31	1.95	≈ 0.1
B36	1.79 ± 1.56	4.04	< 0.01				

[a] IC_{50} values of Btk are an average of at least three independent dose-response curves at K_m ATP (5 nM Btk and 90 μM ATP), mean ± SD. [b] ClogP values are calculated by ChemBioDraw software Ultra 12.0. [c] The solubility was measured by a method as follows: 1.0 mg of the appropriated compound dissolved in 1.0 mL of water at ambient temperature, continuous another 1.0 mL of water was added until the compound was completely dissolved.

It is well known that, molecules with suitable CLogP values and aqueous solubilities will have more chances to own good PK profiles for oral administration and enhance potencies *in vivo* [24-25]. Smith C.R. et al also claimed that CLogP values ranging from 0.5 to 3 were the best for oral administration [26]. Thus, we calculated ClogP values for selected compounds by ChemBioDraw software Ultra 12.0, and determined their solubilities in water at ambient temperature. Similar to ibrutinib, compounds substituted with 4-phenoxyphenyl (**B1**, **B25**, **B27**, **B29**, **B31**, **B32**, **B35 and B36**) or 4-(benzyloxy)phenyl (**B2**) have high ClogP values up to 4, along with poor aqueous solubilities less than 0.01 mg/mL, which may result in unfavorable bioavailability. In our previous studies, candidate compounds with excellent enzymatic potencies but low aqueous solubilities or poor bioavailabilities had demonstrated that they could not enter into further *in vivo* tests or achieve ideal treatment outcomes in animal models. Satisfying our aim for developing this series compounds, benzo[*d*][1,3]dioxol-5-yl derivatives, such as **B16**, **B28**, **B37** and **B38**, exhibited proper ClogP values (1.91~3.06) and aqueous solubilities (≈ 0.1 mg/mL) meeting with the concept of drug-like physical chemical criteria, which promised favorable PK properties to enhance the potencies *in vivo*.

3.2 Cytotoxicity assay

Cytotoxicity to normal cells is often used to evaluate the preliminary toxicities of compounds. Since one of the most important side effects of ibrutinib is renal toxicity, the inhibitory activities against HEK293 cells for selected compounds were assessed

using MTT assay. As shown in **Table 4**, compounds with vinylsulfonyl (**B31**, **B33**, **B36** and **B38**) as electrophilic warhead, as well as **B25** and **B27**, exhibited high toxicities to HEK293 cells with IC_{50} values below 3 μM, indicating that they might result in renal impairment. Fortunately, compound **B16** displayed weaker cytotoxicity than ibrutinib to HEK293 cells. The similar results were also observed in another two normal cell lines of LO2 and THP-1. As a whole, **B16** showed the minimal cytotoxicity that nearly two-fold reduced than ibrutinib on normal cell lines.

Table 4. Cytotoxicity for selected compounds (IC_{50} / μM) [a]

Comp.	HEK293	LO2	THP-1	Comp.	HEK293	LO2	THP-1
ibrutinib	19.3 ± 1.2	17.4 ± 0.5	20.1 ± 0.7	**B31**	2.7 ± 0.5	3.2 ± 0.4	3.3 ± 0.4
B1	13.3 ± 0.9	16.0 ± 1.1	16.7 ± 1.0	**B32**	4.8 ± 0.8	6.6 ± 0.9	3.2 ± 1.1
B16	34.2 ± 1.9	31.3 ± 2.1	38.9 ± 1.5	**B33**	2.5 ± 0.4	3.2 ± 0.4	3.7 ± 0.7
B25	2.9 ± 0.2	11.7 ± 1.9	8.8 ± 1.0	**B35**	11.2 ± 1.1	10.9 ± 1.6	15.7 ± 2.2
B27	1.3 ± 0.2	14.2 ± 2.1	10.7 ± 1.5	**B36**	1.6 ± 0.2	19.1 ± 3.5	18.3 ± 2.7
B29	10.2 ± 1.6	15.2 ± 2.0	18.9 ± 2.8	**B38**	2.8 ± 0.3	10.1 ± 2.1	14.4 ± 0.9

[a] IC_{50} = compound concentration required to inhibit cell proliferation by 50%. Data are expressed as the mean ± SD from the dose-response curves of at least three independent experiments.

3.3 Kinase selectivity profile for compound B16

In consideration of the overall profiles of those compounds, **B16** was selected to further investigation because of its good enzymatic potency, low cytotoxicity and suitable physical chemical properties. The kinase selectivity profile for **B16** was first detected over the closely related Tec and Src family kinases [27-28], as well as kinases that carry a thiol in an analogous position to Cys481 of Btk [16]. A summary of data for kinases screen set was listed in **Table 5**. Unlike ibrutinib, **B16** only exhibited good inhibition to Btk with an IC_{50} value of 21.7 nM, moderately inhibited Bmx (IC_{50} = 61.5 nM) and several other kinases (IC_{50} > 145.0 nM), and had no

inhibition to EGFR, ErbB2, ErbB4, Itk and JAK3 (IC_{50} > 10000 nM). Since irreversible inhibitors can bring unexpected off-target toxicities resulting from the potential of covalently binding to non-target and achieving the drug protein conjugate [13]. Thus, irreversible Btk inhibitors with high kinase selectivity will be more suitable to fulfill the treatment need of non-life-threatening RA disease. Although less potent than ibrutinib on Btk, **B16** was identified as a relatively highly selective Btk inhibitor that could be safer for RA treatment than ibrutinib.

Table 5. Inhibition efficacy and selectivity among different kinases by **B16** (IC_{50} / nM)

kinase	B16 [a]	Ibrutinib [31]	kinase	B16 [a]	Ibrutinib [31]
Btk[*]	21.7	0.5	**MKK6**	>10000	n.f.
Bmx[*]	61.5	0.8	**Fgr**[#]	657.4	2.3
Tec[*]	210.6	78	**Frk**[#]	1129.3	29.2
Itk[*]	>10000	10.7	**Fyn**[#]	1007.8	96
Txk[*]	330.7	n.f.	**Lck**[#]	636.5	33.2
Blk[*#]	503.7	0.5	**Lyn**[#]	259.0	200
EGFR[*]	>10000	5.6	**Src**[#]	1000.9	171
ErbB2[*]	>10000	9.4	**Yes**[#]	145.9	6.5
ErbB4[*]	>10000	n.f.	**Hck**[#]	1111.6	3.7
MKK7β[*]	>10000	n.f.	**Flt3**	>10000	73
JAK3[*]	>10000	16.1	**Fms**	>10000	5545
JAK1	>10000	>10000	**mTOR**	>10000	n.f.
JAK2	>10000	>10000	**p70S6K**	>10000	n.f.
CaMKI	>10000	n.f.	**PKC**	>10000	n.f.
CaMKII	>10000	n.f.	**Ret**	639.8	36.5
CaMKIV	>10000	n.f.	**Rsk1**	>10000	>10000
CaMKK1	>10000	n.f.	**Rsk2**	>10000	n.f.
CaMKK2	>10000	n.f.	**Rsk3**	>10000	n.f.
CSK	>10000	2.3	**Rsk4**	>10000	n.f.
GSK3α/β	>10000	n.f.	**Tak**	>10000	n.f.
MEK1	>10000	n.f.	**Syk**	>10000	>10000

MEK2	>10000	>10000	**Trka**	>10000	n.f.
MEKK2	>10000	n.f.	**Trkb**	>10000	n.f.
MEKK3	>10000	n.f.	**Trkc**	>10000	n.f.
MKK4	>10000	n.f.	**PI3K**	>10000	>10000

[a] IC_{50} values are an average of at least two independent dose-response curves in the presence of 10 μM ATP. [*]Kinases that contain a cysteine residue aligning with Cys481 in Btk. [#]Kinases that belong to Src family. n.f. = not found.

3.4 Kinetics study for compound B16

Given that the inactivation of Btk by irreversible inhibitor **B16** may occur through a two-step process that begins with reversible binding of **B16** to Btk followed by irreversible covalent bond formation with the thiol of Cys481, we next examined the overall inactivation constant ($K_{on} = K_{inact} / K_i$, second-order rate constant) of **B16** using an activity-based, time-dependent assay, which is highly dependent on the inhibitor concentration and its chemical property. As shown in **Figure 4A**, the conversion % curves describing the activity of Btk presented a concentration-dependent and time-dependent manner, which were used to determine Kobs (exponential rate constant) at each inhibitor (**B16**) concentration. As we known, a plot is made of Kobs versus inhibitor concentration, if this plot is linear, the slope is K_{on} and the y-intercept is K_{off}. As displayed in **Figure 4B**, **B16** was slowly on binding to Btk with a K_{on} value of 0.000578 $nM^{-1}.min^{-1}$ and a K_{off} value of 0.03116 $nM^{-1}.min^{-1}$ (**Figure 4**).

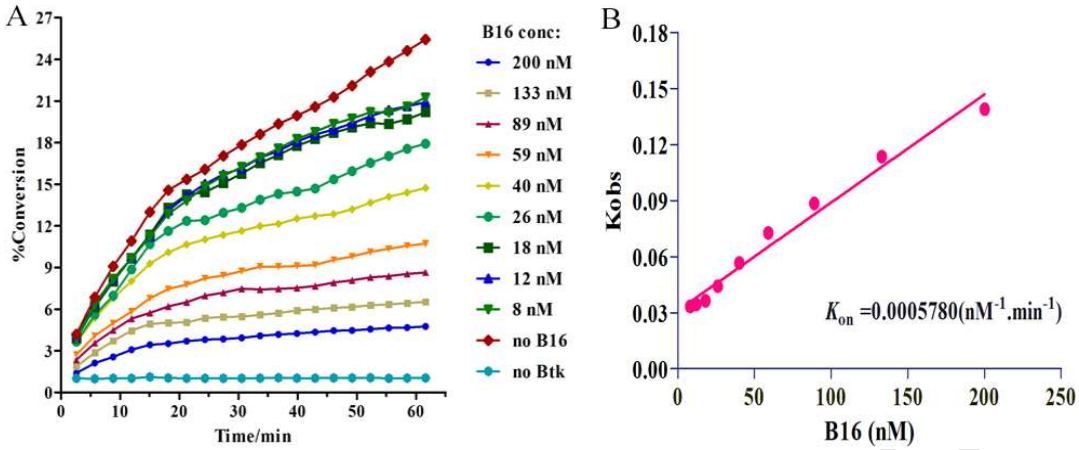

Figure 4. Kinetics study for compound **B16**. A: The conversion % of Btk after incubated with different concentrations of compound B16. B: The K_{on} (K_{inact} / K_i) value determined for **B16**, K_i: reversible binding affinity; K_{inact}: inactivation rate constant.

3.5 Inhibition of hERG current assay for compound B16

Some drugs that induce prolongation of the cardiac action potential and manifest as a prolongation of the QT interval on an electrocardiogram, have been withdrawn from market because of their association with a potentially fatal cardiac arrhythmia called Torsades de Pointes [29-30]. During past decades, numerous efforts to reduce the incidence of sudden cardiac death have focused largely on assays using the K^+ channel, encoded by the human ether-a-go-go-related gene (hERG), as a standard component of preclinical safety testing [29-30]. The inhibition of hERG potassium current by **B16** was tested using automated QPatch clamp technology in CHO cells. **B16** inhibited hERG current in a concentration dependent manner with an IC_{50} value of 11.10 μM, which is 11 folds greater than the IC_{50} obtained by ibrutinib (0.97 μM) [26], suggesting that **B16** showed very low potential of blocking the hERG channel and low risk for cardiotoxicity.

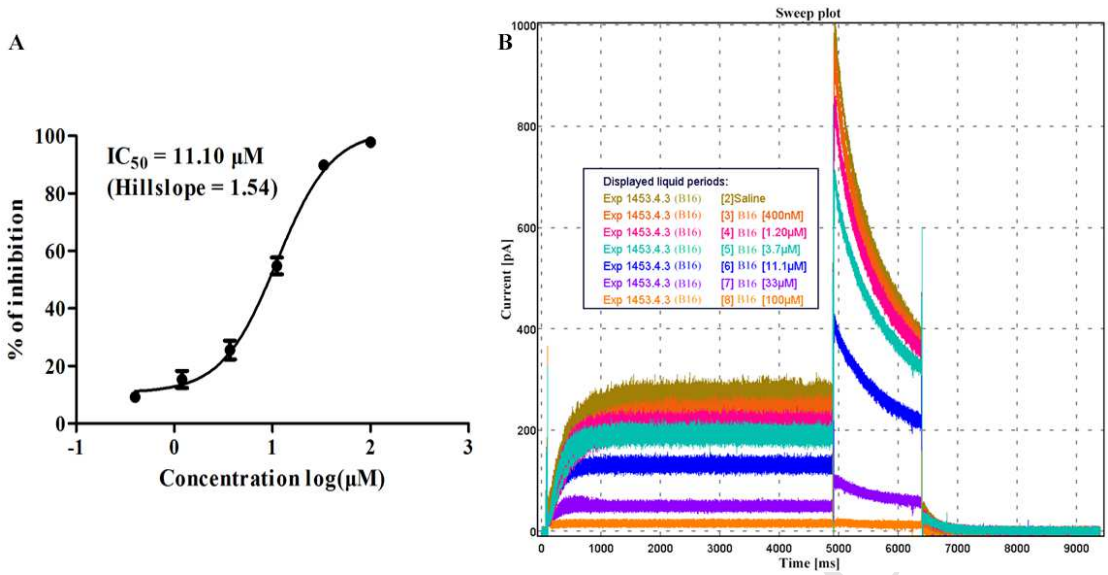

Figure 5. The inhibition of hERG current by **B16**. (**A**). Dose-dependent response curve of **B16** inhibiting hERG potassium current. (**B**) Raw current traces responding to vehicle and six doses of **B16**.

3.6 Western blot analysis for mediated signaling pathway of Btk by B16

B16 was examined in a series of **B** lymphoma cells including Daudi cells (Btk overexpression), U2932 and Raji cells to determine its effect on the Btk mediated cellular signaling pathway by western blot analysis. As illustrated in **Figure 6**, **B16** potently inhibited Btk Y223 *auto*-phosphorylation in all tested cells in a concentration dependent manner, but did not affect the *trans*-phosphorylation site Y551 (Syk phosphorylation site), which were consistent with the enzymatic results. As expected, **B16** also exhibited inhibition to the Btk downstream mediator PLCγ2 Y1217 phosphorylation in respective cells. Among these cell lines, **B16** showed the most favorable suppression on the Btk mediated signaling pathway in Daudi cells, of which 0.1 μM began to reduce Btk Y223 *auto*-phosphorylation and 0.3 μM started to inhibit PLCγ2 Y1217 phosphorylation, while had moderated inhibition in U2932 cells and the least inhibition in Raji cells.

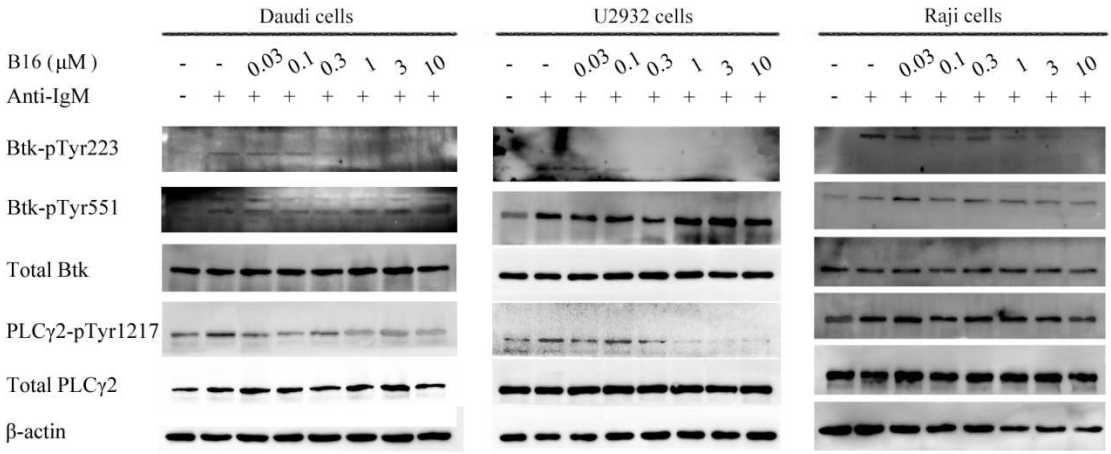

Figure 6. Western blot analysis for compound **B16**'s effect on the Btk mediated signaling pathway in Daudi, U2932 and Raji cells.

3.7 Pharmacokinetic properties of B16

In rat pharmacokinetic study, **B16** exhibited reasonable maximum concentration (C_{max} = 257.82 μg/L), acceptable oral clearance rate (Cl = 2.75 L/h/kg), favorable half-life ($t_{1/2}$ = 7.04 h) and good bioavailability (F = 49.15%) at an oral dose of 3 mg/kg, which was much higher than the oral bioavailability of ibrutinib ranging from 18 to 23% in a variety of rats [18]. This might be attributed to the significant improvement of its ClogP and aqueous solubility.

Table 6. Pharmacokinetic parameters for compound **B16** in SD rat

	Intravenous	**Oral**
dose (mg/kg)	3	3
C_{max} (μg/L)	3132.28	257.82
t_{max} (h)	0.11	0.96
$t_{1/2}$ (h)	5.18	7.04
AUC_{0-t} (μg/L*h)	2522.28	1239.63
V, V/F (L/kg)	1.21 (V)	26.15 (V/F)
Cl, Cl/F (L/h/kg)	8.23V(Cl)	2.75 (Cl/F)
F%		**49.15**

Data were mean concentrations in rat plasma (n = 5).

Owing to covalent features, **B16** was found to be stable in liver microsome of various species (**Table 7**). Among them, **B16** exhibited high stability in human live microsome with a half-life of 330.0 min and a low clearance rate of 0.0042 $mg^{-1}\cdot mL\cdot min^{-1}$. In mice liver microsome, **B16** was moderately stable ($t_{1/2}$ = 256.7 min). By comparison, **B16** was relatively rapidly cleared in rat ($t_{1/2}$ = 187.3 min) and monkey ($t_{1/2}$ = 169.0 min) liver microsome. To further investigate the cytochrome P450 activities, the potential of **B16** to inhibit the formation of metabolites by six CYP isoforms (CYP1A2, 3A4, 2C9, 2C19, 2D6 and 2E1) was assessed using human live microsomes and corresponding substrates through metabolism-dependent CYP inhibition assay [34]. As shown in **Table 8**, **B16** displayed a strong inhibition to CYP1A2 (IC_{50} = 0.059±0.01 μM) indicating that it need to be careful if it was combined use of other CYP1A2 metabolism drugs. The activities of CYP3A4 and 2C9, were moderately inhibited by **B16** with IC_{50} values about 3 μM. **B16** displayed very weak inhibition against CYP2C19 and 2D6, and at up to 100 μM didn't inhibit CYP2E1.

Table 7. *In vitro* liver microsome stability expressed as half-lives ($t_{1/2}$) and clearance rates (Cl_{int}) of **B16**

	human	**rat**	**dog**	**mice**	**monkey**
$t_{1/2}$ (min)	330.0	187.3	315.0	256.7	169.0
Cl_{int} ($mg^{-1}\cdot mL\cdot min^{-1}$)	0.0042	0.0074	0.0044	0.0054	0.0082

Table 8. The CYP inhibition of **B16**.

CYP450	**1A2**	**3A4**	**2C9**	**2C19**	**2D6**	**2E1**
IC_{50} (μM)	0.06±0.01	3.19±0.05	3.54±0.04	41.66±0.03	60.1±0.05	1308027.51±0.07

CYP = cytochrome P450. HLM CYP assay. IC_{50} values are an average of three independent dose-response curves.

3.8 Anti-arthritic activity evaluation of B16 in CIA model.

With a desirable activity and selectivity profile, a relatively clear liability profile, low toxicity, as well as favorable pharmacokinetic properties, **B16** was further evaluated for anti-arthritis efficacy in the mice model of CIA. All mice that appeared serious arthritis and reached a clinical score about 4.0 ± 0.3 were randomly divided into 4 groups based on the weight. On the basis of enzymatic potencies and bioavailability of **B16**, as well as making reference of ibrutinib's treatment in CIA mice, treatment groups were orally administrated **B16** and ibrutinib at a dosage of 20 mg/kg once a day, respectively. As shown in **Figure 7**, both treated groups suppressed arthritis progression without any significant changes of body weight (**Figure S1**). The clinical scores in mice treated with **B16** were reduced to 2.71 ± 1.38 on day 30, a little lower than that of ibrutinib (2.87 ± 1.36). The forelimb and hindlimb in model mice without any treatment were both severely swollen (**Figure 7B**). Treatment groups potently inhibited edema formation and the increased paw thickness, suggesting that **B16** could become an efficacious treatment for RA.

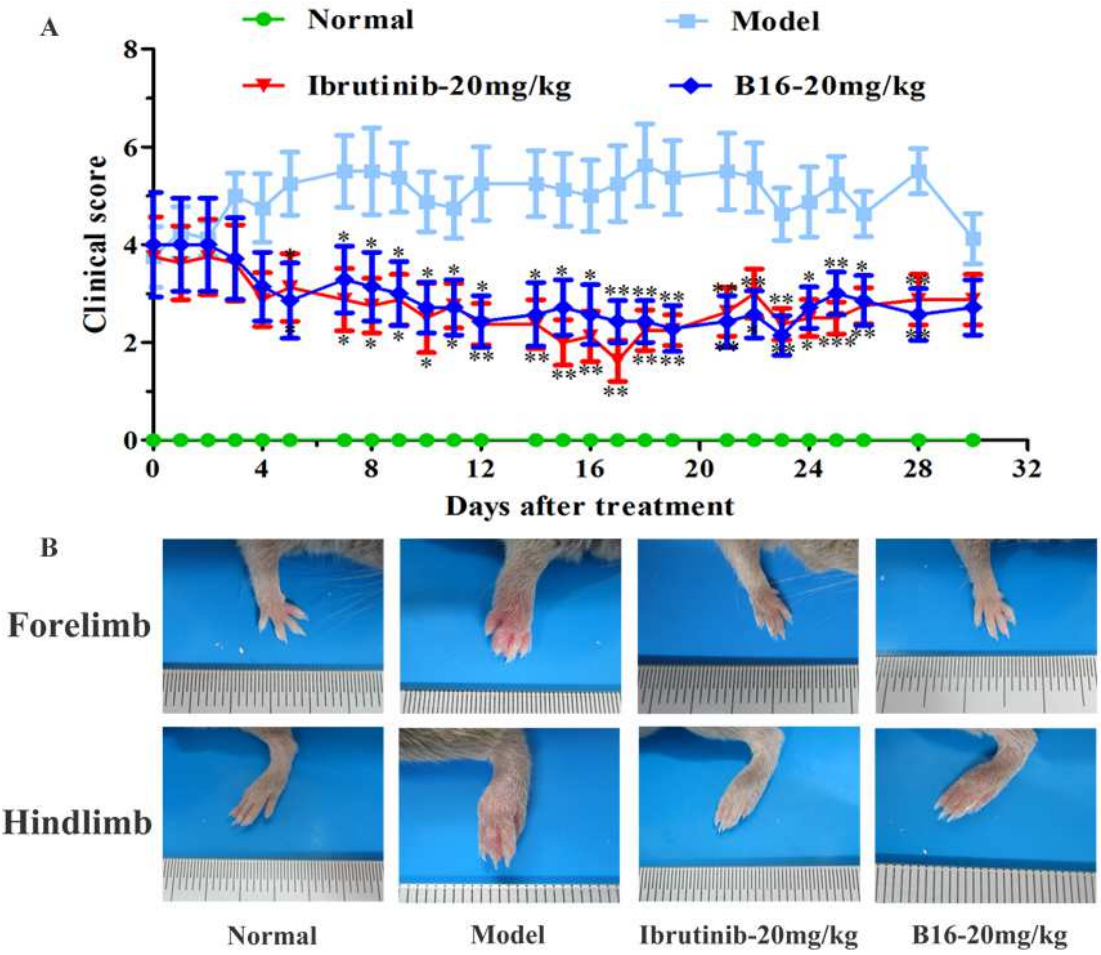

Figure 7. **B16** improves clinical symptoms in developing disease in a mice CIA model. Arthritis was induced in the mice immunization with type II collagen. The animals were randomized according to body weight, and oral treatment with **B16** (20 mg/kg) or ibrutinib (20 mg/kg) was initiated on day 36; n = 8 for all group. (**A**) Clinical arthritic scores in each group, **B16** treatment led to a significant lower arthritis score than recorded for the model group. *P< 0.05; **P < 0.01; ***P< 0.001 versus model control. (**B**) Forelimbs and hindlimbs of each group mice after treatment with **B16** and ibrutinib.

Subsequently, single oral dose toxicity test of **B16** was conducted in BALB/c mice, which was important in the early stage of drug development. 6 female mice and 6 male mice were oral administration with **B16** at a dose of 2.0 g/kg, which was referenced to ibrutinib [18]. All mice were observed to be survival and healthy with

free movement, normal behavior, and sensitive to light, sound and other stimulations, and without any clinical signs observed in the 7 consecutive days. Histopathology study also demonstrated no histopathological changes in heart, liver, spleen, lung and kidney (**Figure S2**), indicating that **B16** was safe and suitable for *in vivo* application.

4. Conclusion

In summary, we have described the identification of irreversible Btk inhibitors bearing 7*H*-pyrrolo[2,3-*d*]pyrimidin-4-amine core. SAR studies of the different parts of those inhibitors led to the identification of several lead compounds with excellent inactivation to Btk, including **B1**, **B16**, **B25**, **B27**, **B29**, **B31**, **B32**, **B33**, **B35**, **B36** and **B38**. However, most of them revealed good inhibition against HEK293 cells, even better than ibrutinib, which would lead to severe kidney damage. Among them, **B16** not only displayed preference towards Btk over closely related kinases *in vitro*, but also low cytotoxicity towards HEK293 cells, as well as LO2 and THP-1 cells. Moreover, **B16** could not potently inhibit hERG current with an IC_{50} value up to 11.10 μM, suggesting that **B16** showed little or no potential to block the hERG channel. Western blot analysis also revealed that the inhibition of B16 to Btk was contributed to its inhibition to Btk Y223 *auto*-phosphorylation and PLCγ2 Y1217 phosphorylation. Combining favorable physicochemical properties, kinase selectivity, pharmacokinetic profiles and low toxicity, **B16** exhibited potent anti-arthritis activity and similar efficacy to ibrutinib in reducing paw thickness in CIA mice. Therefore, **B16** is a potent, selective, safe and durable inhibitor of Btk and has the potential to an efficacious treatment for arthritis.

Experimental section.

Chemistry. Hydrogen nuclear magnetic resonance(^{1}H NMR) spectra were recorded at 400 MHz while carbon nuclear magnetic resonance(^{13}C NMR) spectra were recorded at 101 MHz on a Varian spectrometer (Varian, Palo Alto, CA) model Gemini 400 and reported in parts per million. Chemical shifts (δ) are quoted in ppm relative to

tetramethylsilane (TMS) as an internal standard, where (δ) TMS = 0.00 ppm. The multiplicity of the signal is indicated as s, singlet; brs, broad singlet; d, doublet; t, triplet; q, quartet; m, multiplet, defined as all multi peak signals where overlap or complex coupling of signals makes definitive descriptions of peaks difficult. Mass spectra (MS) were measured by MALDI Q-TOF Priemier mass spectrometer (Micromass, Manchester, UK). Room temperature is within the range 20-25 °C. The purity was analyzed by HPLC system (Waters 2695, separations module) with a photodiode array detector (Waters 2996, Milford, MA, U.S.), and the chromatographic column was a reversed phase C18 column (Waters, 150 mm × 4.6 mm, i.d. 5 μm). All compounds were supplied in HPLC degree methanol with 10 μL, which was injected on a partial loop, with gradient elution with methanol/H_2O (60/40, v/v) to methanol/H_2O (95/5, v/v) at a flow rate of 1 mL/min. The purity of all tested compounds was ≥ 95% according to our analytical HPLC method.

General procedure for the preparation of compound **2**. Methanesulfonyl chloride (1.15eq, 6.07 g, 52.9 mmol) was added dropwise to a solution of **1-1** (1eq, 10.0 g, 46.4 mmol) and triethylamine (1.5eq, 7.11 g, 70.3 mmol) in methylene chloride (120 mL) in an ice bath. After 1 h, the mixture was evaporated. The residue was diluted with EtOAc and water, extracted with EtOAc, washed with water, brine, then dried over Na_2SO_4, filtered, and finally evaporated to give the crude product **2** as pale yellow solid (14.84 g, 95.81% yield).

General procedure for the preparation of compound **3**. A mixture of **2** (1eq, 11.72 g, 40 mmol) and lithium bromide (5eq, 17.20 g, 200 mmol) in acetone (80 mL) was heated to reflux overnight. The mixture was evaporated, then the residue was partitioned between EtOAc and water. The organic layer was washed with s brine, dried over Na_2SO_4, filtered, and evaporated to offer the title product **3** as pale yellow oil (9.46 g, 85.40% yield).

General procedure for the preparation of compound **5** and **11**. K_2CO_3 (1.5eq, 5.69 g, 41.25 mmol) was added to a solution of **4** (1eq, 6.98 g, 25 mmol) and **3** (1.1eq, 7.62 g, 27.5 mmol) in DMF (25 mL) at r.t.. The resulting mixture was heated to 80 °C and

stirred for another 3 h. Then the mixture was cooled to r.t. extracted with EtOAc, washed with brine, and dried over anhydrous Na_2SO_4. The organic layer was evaporated and the residue was purified by a flash column to give the product **5** as white solid (6.02 g, 64.20% yield). Intermediate **11** was synthesized following the procedure of preparation **5**.

General procedure for the preparation of compound **6**. A solution of **5** (1eq, 4.58 g, 10 mmol) and NH_4OH (8 mL) in 1.4-dioxane (30 mL) was stirred in an autoclave at 100 °C overnight. The mixture was allowed to cool to r.t. and concentrated *in vacuo*, then water (30 mL) was added. The mixture was subjected to sonication for 10 min. The resulting solid was collected by filtration and dried *in vacuo* to afford the desired product **6** as off-white solid (~75% yield).

General procedure of Suzuki coupled reaction for the preparation of compounds **7** and **12**. To a mixture of halides (1eq, 5 mmol), boric acid derivatives (1.1eq, 5.5 mmol), $PdCl_2$(dppf) (0.1eq, 365.85 mg, 0.5 mmol) and K_2CO_3 (3eq, 2.07 g, 15 mmol) in a 100 mL reaction vial under vacuum, 75 mL of H_2O/1,4-dioxane (1/8, v/v) was added via a syringe. The mixture was re-fed with N_2 and heated to 100 °C for 3-4 h. Then the solvent was evaporated. The residue was dissolved in EtOAc/H_2O, extracted with EtOAc, washed with water, brine, dried over Na_2SO_4, filtered, and evaporated. The residue was purified with flash column chromatography to afford coupled product **7** as yellow solids (~50% yield). Intermediate **12** was synthesized according to the procedure for the preparation of **7**.

General procedure for the preparation of compounds **8** and **13**. 4M HCl in 1,4-dioxane (3eq) was added to a stirred solution of **7** (1eq) in 1,4-dioxane at r.t.. The resulting solution was heated to 55 °C under stirring overnight. The corresponding hydrochlorides **8** were obtained by filtration as light yellow solid (~60% yield). Intermediate **13** was prepared according to the procedure of preparation **8**.

General procedure for the preparation of compounds **10**. NIS (1.1eq, 4.95 g, 22 mmol) was slowly added into the mixture of **9** (1eq, 2.70 g, 20 mmol) and DMF (50 mL) at r.t.. The reaction mixture was continued stirred at r.t. overnight. The solvent was

removed *in vacuo* and water was added. The mixture was subjected to sonication for 10 min. The precipitate was collected by filtration, rinsed with water, and dried. The solid **10** was used for the next step without further purification (5.01 g, 96% yield).

General procedure for the preparation of compounds **B1-B30**, **B35** and **B37**. A mixture of piperidine hydrochloride (1eq, 0.3 mmol) and DIEA (5eq, 193.5 mg, 1.5 mmol) in dry DMF (2 mL) was added acryloyl chloride (1.3eq, 35.3 mg, 0.39 mmol) in an ice bath. The reaction mixture was stirred at r.t. for another 1 h and quenched with cold water. The mixture was extracted with DCM, washed with brine, dried over anhydrous Na_2SO_4, and concentrated under reduced pressure. Purification the residue by a flash column gave target compounds as white solids (~37% yield).

General procedure for the preparation of compounds **B31**, **B33**, **B36** and **B38**. A mixture of piperidine hydrochloride (1eq, 0.3 mmol) and DIEA (5eq, 193.5 mg, 1.5 mmol) in dry DCM (6 mL) was added 2-chloroethanesulfonyl chloride (1.3eq, 63.6 mg, 0.39 mmol) in an ice bath. The reaction mixture was stirred at r.t. for another 1 h and quenched with cold water. The mixture was extracted with DCM, washed with brine, dried over anhydrous Na_2SO_4, and concentrated under reduced pressure. Purification the residue using a flash column gave target compounds as white solids (~30% yield).

General procedure for the preparation of compounds **B32** and **B34**. The solution of *trans*-4-dimethylaminocrotonic acid hydrochloride (1.5eq, 74.5 mg; 0.45 mmol) and DIEA (1.5eq, 0.07 mL; 0.45 mmol) in DCM (5 mL) was stirred in an ice bath for about 10 min, then slowly added mixture of piperidine hydrochloride (1eq, 0.3 mmol) and DIEA (5eq, 193.5 mg, 1.5 mmol) in DCM (6 mL). The reaction mixture was stirred at r.t. overnight. The solvent was removed by under reduced pressure, and the residue was purified using a flash column to give target compounds as white solids (~30% yield).

1-(4-((4-Amino-5-(4-phenoxyphenyl)-7*H*-pyrrolo[2,3-*d*]pyrimidin-7-yl)methyl)piperidin-1-yl)prop-2-en-1-one (B1). Purity: HPLC 95.9%. ^{1}H NMR (400 MHz, DMSO-d_6): δ 8.14 (d, J = 5.5 Hz, 1H), 7.47 (d, J = 8.6 Hz, 2H), 7.42 (t, J = 7.9 Hz,

2H), 7.31 (s, 1H), 7.16 (t, *J* = 7.4 Hz, 1H), 7.13-7.06 (m, 4H), 6.77 (dd, *J* = 16.7, 10.5 Hz, 1H), 6.07 (dd, *J* = 16.7, 2.4 Hz, 3H), 5.63 (dd, *J* = 10.4, 2.4 Hz, 1H), 4.37 (t, *J* = 12.2 Hz, 1H), 4.08 (d, *J* = 7.2 Hz, 2H), 4.02 (d, *J* = 12.5 Hz, 1H), 2.98 (t, *J* = 12.2 Hz, 1H), 2.59 (t, *J* = 12.2 Hz, 1H), 2.23-2.12 (m, 1H), 1.55 (d, *J* = 12.0 Hz, 2H), 1.11 (dd, *J* = 33.6, 13.3 Hz, 2H). ^{13}C NMR (101 MHz, DMSO-d_6): δ 164.61, 157.76, 157.20, 155.94, 152.08, 150.93, 130.54, 130.47, 130.38, 129.01, 127.42, 124.34, 123.94, 119.62, 119.11, 114.84, 100.27, 49.33, 45.20, 41.61, 36.84, 30.71, 29.61. MS (ESI), m/z: 454.22 $[M + H]^+$.

1-(4-((4-Amino-5-(4-(benzyloxy)phenyl)-7*H*-pyrrolo[2,3-*d*]pyrimidin-7-yl)methyl)piperidin-1-yl)prop-2-en-1-one (B2). Purity: HPLC 97.0%. ^{1}H NMR (400 MHz, DMSO-d_6): δ 8.13 (s, 1H), 7.48 (d, *J* = 7.1 Hz, 2H), 7.45-7.31 (m, 4H), 7.24 (s, 1H), 7.12 (d, *J* = 8.6 Hz, 2H), 6.77 (dd, *J* = 16.7, 10.5 Hz, 1H), 6.06 (dt, *J* = 15.4, 7.7 Hz, 3H), 5.63 (dd, *J* = 10.5, 2.4 Hz, 1H), 5.15 (s, 2H), 4.39 (d, *J* = 12.4 Hz, 1H), 4.06 (d, *J* = 7.2 Hz, 2H), 4.04-3.95 (m, 1H), 2.98 (t, *J* = 12.3 Hz, 1H), 2.59 (t, *J* = 12.2 Hz, 1H), 2.16 (ddd, *J* = 11.1, 8.7, 5.4 Hz, 1H), 1.55 (d, *J* = 12.0 Hz, 2H), 1.19-1.05 (m, 2H). ^{13}C NMR (101 MHz, DMSO-d_6): δ 164.61, 157.83, 157.74, 152.01, 150.76, 137.55, 130.12, 129.02, 128.93, 128.33, 128.19, 127.65, 127.41, 123.94, 115.76, 115.08, 100.43, 69.77, 49.29, 45.21, 41.61, 36.86, 30.70, 29.61. MS (ESI), m/z: 468.26 $[M + H]^+$.

1-(4-((4-Amino-5-(4-(pyridin-2-yloxy)phenyl)-7*H*-pyrrolo[2,3-*d*]pyrimidin-7-yl)m ethyl)piperidin-1-yl)prop-2-en-1-one (B3). Purity: HPLC 95.8%. ^{1}H NMR (400 MHz, DMSO-d_6): δ 8.19 (dd, *J* = 4.9, 1.9 Hz, 1H), 8.16 (s, 1H), 7.91-7.85 (m, 1H), 7.50 (d, *J* = 8.5 Hz, 2H), 7.36 (s, 1H), 7.23 (d, *J* = 8.5 Hz, 2H), 7.15 (dd, *J* = 7.1, 5.0 Hz, 1H), 7.08 (d, *J* = 8.3 Hz, 1H), 6.78 (dd, *J* = 16.7, 10.5 Hz, 1H), 6.14 (s, 2H), 6.07 (dd, *J* = 16.7, 2.4 Hz, 1H), 5.64 (dd, *J* = 10.5, 2.4 Hz, 1H), 4.39 (d, *J* = 12.5 Hz, 1H), 4.09 (d, *J* = 7.2 Hz, 2H), 4.03 (dd, *J* = 14.1, 6.9 Hz, 1H), 2.99 (t, *J* = 12.4 Hz, 1H), 2.59 (t, *J* = 12.2 Hz, 1H), 2.18 (t, *J* = 7.3 Hz, 1H), 1.54 (s, 2H), 1.17-1.07 (m, 2H). MS (ESI), m/z: 455.20 $[M + H]^+$.

1-(4-((4-Amino-5-(4-(morpholine-4-carbonyl)phenyl)-7*H*-pyrrolo[2,3-*d*]pyrimidi

n-7-yl)methyl)piperidin-1-yl)prop-2-en-1-one (B4). Purity: HPLC 96.0 %. ^{1}H NMR (400 MHz, DMSO-d_6): δ 8.17 (s, 1H), 7.51 (q, J = 8.0 Hz, 4H), 7.42 (s, 1H), 6.77 (dd, J = 16.6, 10.5 Hz, 1H), 6.24 (s, 2H), 6.06 (dd, J = 16.7, 2.1 Hz, 1H), 5.63 (dd, J = 10.5, 2.1 Hz, 1H), 4.39 (d, J = 11.4 Hz, 1H), 4.09 (d, J = 7.0 Hz, 2H), 4.05-3.97 (m, 1H), 3.62 (s, 8H), 3.00 (t, J = 11.7 Hz, 1H), 2.59 (t, J = 11.7 Hz, 1H), 2.18 (s, 1H), 1.55 (d, J = 10.3 Hz, 2H), 1.16 (dd, J = 16.5, 9.3 Hz, 2H). ^{13}C NMR (101 MHz, DMSO-d_6): δ 169.46, 164.62, 157.61, 151.95, 151.15, 136.43, 133.84, 129.01, 128.55, 128.33, 127.43, 125.18, 114.95, 100.00, 66.62, 49.42, 45.20, 41.61, 36.81, 30.69, 29.59. MS (ESI), m/z: 475.32 $[M + H]^+$.

1-(4-((5-([1,1'-Biphenyl]-4-yl)-4-amino-7*H*-pyrrolo[2,3-*d*]pyrimidin-7-yl)methyl)piperidin-1-yl)prop-2-en-1-one (B5). Purity: HPLC 97.2%. ^{1}H NMR (400 MHz, DMSO-d_6): δ 8.17 (s, 1H), 7.79 (d, J = 8.3 Hz, 2H), 7.76 – 7.71 (m, 2H), 7.57 (d, J = 8.3 Hz, 2H), 7.49 (t, J = 7.7 Hz, 2H), 7.41 (s, 1H), 7.38 (t, J = 7.3 Hz, 1H), 6.77 (dt, J = 17.5, 8.7 Hz, 1H), 6.19 (s, 2H), 6.06 (dt, J = 9.3, 4.6 Hz, 1H), 5.64 (dd, J = 10.5, 2.4 Hz, 1H), 4.40 (d, J = 12.5 Hz, 1H), 4.10 (d, J = 7.2 Hz, 2H), 4.06-3.96 (m, 1H), 2.99 (t, J = 11.9 Hz, 1H), 2.60 (t, J = 12.1 Hz, 1H), 2.25-2.11 (m, 1H), 1.57 (d, J = 12.2 Hz, 2H), 1.17 (dd, J = 14.0, 6.9 Hz, 2H). ^{13}C NMR (101 MHz, DMSO-d_6): δ 164.62, 157.79 152.11, 151.11, 140.16, 138.64, 134.33, 129.46, 129.30, 129.01, 127.90, 127.66, 127.42, 126.98, 124.71, 115.09, 100.21, 49.40, 45.22, 41.64, 36.85, 30.72, 29.64. MS (ESI), m/z: 438.18 $[M + H]^+$.

1-(4-((4-Amino-5-(3-chlorophenyl)-7*H*-pyrrolo[2,3-*d*]pyrimidin-7-yl)methyl)piperidin-1-yl)prop-2-en-1-one (B6). Purity: HPLC 98.0%. ^{1}H NMR (400 MHz, DMSO-d_6) : δ 8.15 (d, J = 5.6 Hz, 1H), 7.52-7.50 (m, 1H), 7.48 (d, J = 7.8 Hz, 1H), 7.44 (s, 1H), 7.42 (dd, J = 6.4, 1.4 Hz, 1H), 7.40-7.36 (m, 1H), 6.77 (dd, J = 16.7, 10.5 Hz, 1H), 6.25 -5.99 (m, 3H), 5.64 (dd, J = 10.5, 2.4 Hz, 1H), 4.06 (d, J = 7.2 Hz, 2H), 3.91 (d, J = 12.6 Hz, 2H), 2.67 (d, J = 1.8 Hz, 2H), 2.05 (ddd, J = 11.4, 7.6, 3.7 Hz, 1H), 1.48 (d, J = 9.4 Hz, 2H), 1.14-1.04 (m, 2H). ^{13}C NMR (101 MHz, DMSO-d_6): δ 164.63, 157.77, 152.21, 151.21, 137.33, 133.95, 131.13, 129.03, 128.36, 127.38, 127.33, 126.72, 125.34, 114.12, 100.01, 49.42, 45.21, 41.61, 36.79, 30.68,

29.60. MS (ESI), m/z: 396.21 $[M + H]^+$.

1-(4-((4-Amino-5-(4-fluorophenyl)-7*H*-pyrrolo[2,3-*d*]pyrimidin-7-yl)methyl)piperidin-1-yl)prop-2-en-1-one (B7). Purity: HPLC 98.5%. ^{1}H NMR (400 MHz, DMSO-d_6): δ 8.15 (s, 1H), 7.49 (dd, J = 8.6, 5.5 Hz, 2H), 7.33 (s, 1H), 7.30 (t, J = 8.9 Hz, 2H), 6.77 (dd, J = 16.7, 10.5 Hz, 1H), 6.27 -5.98 (m, 3H), 5.64 (dd, J = 10.5, 2.4 Hz, 1H), 4.39 (d, J = 12.1 Hz, 1H), 4.07 (d, J = 7.2 Hz, 2H), 4.05-3.97 (m, 1H), 2.98 (t, J = 11.9 Hz, 1H), 2.59 (t, J = 11.9 Hz, 1H), 2.17 (ddd, J = 14.8, 7.4, 3.5 Hz, 1H), 1.55 (d, J = 12.0 Hz, 2H), 1.18-1.08 (m, 2H). ^{13}C NMR (101 MHz, DMSO-d_6-d_6): δ 164.61, 162.93, 160.51, 157.74, 152.11, 150.95, 131.53, 130.74, 129.01, 127.41, 124.55, 116.30, 116.09, 114.43, 100.25, 49.34. 45.21, 41.61, 36.84, 30.70, 29.61. MS (ESI), m/z: 380.04 $[M + H]^+$.

1-(4-((4-Amino-5-(4-(trifluoromethoxy)phenyl)-7*H*-pyrrolo[2,3-*d*]pyrimidin-7-yl)methyl)piperidin-1-yl)prop-2-en-1-one (B8). Purity: HPLC 97.2%. ^{1}H NMR (400 MHz, DMSO-d_6): δ 8.16 (s, 1H), 7.61-7.53 (m, 2H), 7.45 (d, J = 8.0 Hz, 2H), 7.40 (s, 1H), 6.77 (dd, J = 16.7, 10.5 Hz, 1H), 6.15 (s, 2H), 6.06 (dd, J = 16.7, 2.4 Hz, 1H), 5.63 (dd, J = 10.5, 2.4 Hz, 1H), 4.38 (d, J = 13.0 Hz, 1H), 4.08 (d, J = 7.2 Hz, 2H), 4.05-3.98 (m, 1H), 2.98 (t, J = 12.5 Hz, 1H), 2.59 (t, J = 11.9 Hz, 1H), 2.23-2.10 (m, 1H), 1.55 (d, J = 12.3 Hz, 2H), 1.12 (t, J = 20.2 Hz, 2H). ^{13}C NMR (101 MHz, DMSO-d_6): δ 164.62, 157.79, 152.18, 151.16, 147.53, 134.56, 130.45, 129.01, 127.42, 125.11, 121.97, 114.13, 100.09, 49.39, 45.20, 41.59, 36.81, 30.68, 29.59. MS (ESI), m/z: 446.17 $[M + H]^+$.

1-(4-((4-Amino-5-(4-(trifluoromethyl)phenyl)-7*H*-pyrrolo[2,3-*d*]pyrimidin-7-yl)methyl)piperidin-1-yl)prop-2-en-1-one (B9). Purity: HPLC 96.7%. ^{1}H NMR (400 MHz, DMSO-d_6): δ 8.17 (s, 1H), 7.80 (d, J = 8.2 Hz, 2H), 7.67 (d, J = 8.1 Hz, 2H), 7.49 (s, 1H), 6.77 (dd, J = 16.7, 10.5 Hz, 1H), 6.23 (s, 2H), 6.06 (dd, J = 16.7, 2.4 Hz, 1H), 5.64 (dd, J = 10.5, 2.4 Hz, 1H), 4.39 (d, J = 12.2 Hz, 1H), 4.10 (d, J = 7.2 Hz, 2H), 4.06-3.98 (m, 1H), 2.98 (t, J = 12.6 Hz, 1H), 2.59 (t, J = 12.1 Hz, 1H), 2.23-2.12 (m, 1H), 1.55 (d, J = 12.1 Hz, 2H), 1.13 (dd, J = 28.9, 18.5 Hz, 2H). ^{13}C NMR (101 MHz, DMSO-d_6): δ 164.62, 157.83, 152.29, 151.44, 139.39, 129.15, 129.01, 127.42,

126.23, 126.19, 125.77, 114.26, 99.92, 49.45, 45.20, 41.59, 36.80, 30.68, 29.58. MS (ESI), m/z: 430.19 $[M + H]^+$.

1-(4-((4-Amino-5-(5-fluoropyridin-2-yl)-7*H*-pyrrolo[2,3-*d*]pyrimidin-7-yl)methyl) piperidin-1-yl)prop-2-en-1-one (B10). Purity: HPLC 96.0%. ^{1}H NMR (400 MHz, DMSO-d_6): δ 8.23 (d, J = 2.0 Hz, 1H), 8.14 (s, 1H), 7.77 (dd, J = 8.5, 2.4 Hz, 1H), 7.33 (s, 1H), 6.91 (d, J = 8.5 Hz, 1H), 6.78 (dd, J = 16.7, 10.5 Hz, 1H), 6.11 (s, 2H), 6.07 (dd, J = 16.7, 2.2 Hz, 1H), 5.64 (dd, J = 10.4, 2.3 Hz, 1H), 4.39 (d, J = 13.0 Hz, 1H), 4.07 (d, J = 7.1 Hz, 2H), 4.05-3.99 (m, 1H), 2.98 (t, J = 12.5 Hz, 1H), 2.59 (t, J = 12.5 Hz, 1H), 2.23-2.12 (m, 1H), 1.55 (d, J = 12.3 Hz, 2H), 1.14 (d, J = 12.3 Hz, 2H). ^{13}C NMR (101 MHz, DMSO-d_6): δ 164.62, 162.90, 157.86, 152.13, 151.04, 146.20, 139.76, 129.02, 127.42, 124.53, 124.35, 111.61, 111.01, 100.29, 53.66, 49.36, 45.18, 36.85, 30.72, 29.60. MS (ESI), m/z: 381.26 $[M + H]^+$.

1-(4-((4-Amino-5-(4-(methylsulfonyl)phenyl)-7*H*-pyrrolo[2,3-*d*]pyrimidin-7-yl)m ethyl)piperidin-1-yl)prop-2-en-1-one (B11). Purity: HPLC 95.5%. ^{1}H NMR (400 MHz, DMSO-d_6): δ 8.18 (s, 1H), 7.98 (d, J = 8.3 Hz, 2H), 7.71 (d, J = 8.3 Hz, 2H), 7.53 (s, 1H), 6.77 (dd, J = 16.7, 10.5 Hz, 1H), 6.27 (s, 2H), 6.05 (dd, J = 16.7, 2.4 Hz, 1H), 5.64 (dd, J = 10.5, 2.3 Hz, 1H), 4.39 (d, J = 12.4 Hz, 1H), 4.10 (d, J = 7.2 Hz, 2H), 4.07-3.99 (m, 1H), 3.24 (s, 3H), 2.98 (t, J = 12.3 Hz, 1H), 2.59 (t, J = 11.8 Hz, 1H), 2.17 (d, J = 7.3 Hz, 1H), 1.55 (d, J = 11.5 Hz, 2H), 1.19-1.07 (m, 2H). ^{13}C NMR (101 MHz, DMSO-d_6): δ 164.62, 157.84, 152.36, 151.55, 140.40, 138.66, 129.09, 129.01, 127.43, 126.11, 114.16, 99.89, 49.49, 45.20, 44.20, 41.61, 36.79, 30.68, 29.59. MS (ESI), m/z: 440.20 $[M + H]^+$.

1-(4-((4-Amino-5-(4-hydroxyphenyl)-7*H*-pyrrolo[2,3-*d*]pyrimidin-7-yl)methyl)pip eridin-1-yl)prop-2-en-1-one (B12). Purity: HPLC 95.8%. ^{1}H NMR (400 MHz, DMSO-d_6): δ 9.52 (s, 1H), 8.11 (s, 1H), 7.26 (d, J = 8.1 Hz, 2H), 7.18 (s, 1H), 6.86 (d, J = 8.1 Hz, 2H), 6.77 (dd, J = 16.7, 10.5 Hz, 1H), 6.07 (d, J = 16.6 Hz, 3H), 5.64 (d, J = 10.4 Hz, 1H), 4.38 (d, J = 12.0 Hz, 1H), 4.05 (d, J = 7.1 Hz, 2H), 4.01 (d, J = 7.1 Hz, 1H), 2.98 (t, J = 12.2 Hz, 1H), 2.59 (t, J = 12.2 Hz, 1H), 2.21-2.10 (m, 1H), 1.53 (s, 2H), 1.14 (d, J = 16.8 Hz, 2H). ^{13}C NMR (101 MHz, DMSO-d_6): δ 164.61, 157.73,

156.91, 151.95, 150.63, 130.16, 129.02, 127.40, 125.68, 123.58, 116.21, 115.50, 100.49, 49.25, 45.20, 41.61, 36.88, 30.71, 29.63. MS (ESI), m/z: 378.27 $[M + H]^+$.

1-(4-((4-Amino-5-(4-methoxyphenyl)-7*H*-pyrrolo[2,3-*d*]pyrimidin-7-yl)methyl)piperidin-1-yl)prop-2-en-1-one (B13). Purity: HPLC 99.1%. ^{1}H NMR (400 MHz, DMSO-d_6): δ 8.14 (s, 1H), 7.38 (d, J = 8.6 Hz, 2H), 7.24 (s, 1H), 7.04 (d, J = 8.7 Hz, 2H), 6.77 (dd, J = 16.7, 10.5 Hz, 1H), 6.07 (dd, J = 16.7, 2.4 Hz, 3H), 5.64 (dd, J = 10.5, 2.4 Hz, 1H), 4.39 (d, J = 12.1 Hz, 1H), 4.06 (d, J = 7.2 Hz, 2H), 4.01 (dd, J = 15.6, 8.5 Hz, 1H), 3.80 (s, 3H), 2.98 (t, J = 12.2 Hz, 1H), 2.59 (t, J = 12.0 Hz, 1H), 2.22-2.09 (m, 1H), 1.55 (d, J = 11.7 Hz, 2H), 1.18 -1.05 (m, 2H). ^{13}C NMR (101 MHz, DMSO-d_6): δ 164.61, 158.71, 157.74, 152.01, 150.75, 130.12, 129.02, 127.39, 123.88, 115.12, 114.89, 100.43, 55.63, 49.28, 45.21, 41.62, 36.87, 30.71, 29.62. MS (ESI), m/z: 392.17 $[M + H]^+$.

1-(4-((4-Amino-5-(4-ethoxyphenyl)-7*H*-pyrrolo[2,3-*d*]pyrimidin-7-yl)methyl)piperidin-1-yl)prop-2-en-1-one (B14). Purity: HPLC 97.3%. ^{1}H NMR (400 MHz, DMSO-d_6): δ 8.13 (s, 1H), 7.39-7.33 (m, 2H), 7.24 (s, 1H), 7.06-7.00 (m, 2H), 6.78 (dd, J = 16.7, 10.5 Hz, 1H), 6.18 – 5.89 (m, 3H), 5.64 (dd, J = 10.5, 2.4 Hz, 1H), 4.38 (d, J = 12.1 Hz, 1H), 4.07 (dt, J = 6.9, 5.7 Hz, 4H), 4.01 (s, 1H), 2.98 (t, J = 12.2 Hz, 1H), 2.59 (t, J = 12.2 Hz, 1H), 2.21-2.10 (m, 1H), 1.55 (d, J = 11.3 Hz, 2H), 1.35 (t, J = 7.0 Hz, 3H), 1.13 (d, J = 10.6 Hz, 2H). ^{13}C NMR (101 MHz, DMSO-d_6): δ 164.61, 157.99, 157.74, 152.00, 150.74, 130.11, 129.02, 127.41, 127.25, 123.86, 115.35, 115.15, 100.44, 63.54, 49.28, 45.22, 41.61, 36.87, 30.71, 29.61, 15.17. MS (ESI), m/z: 406.25 $[M + H]^+$.

1-(4-((4-Amino-5-(4-(2-methoxyethoxy)phenyl)-7*H*-pyrrolo[2,3-*d*]pyrimidin-7-yl)methyl)piperidin-1-yl)prop-2-en-1-one (B15). Purity: HPLC 96.1%. ^{1}H NMR (400 MHz, DMSO-d_6): δ 8.13 (s, 1H), 7.37 (d, J = 8.6 Hz, 2H), 7.24 (s, 1H), 7.05 (d, J = 8.6 Hz, 2H), 6.78 (dd, J = 16.7, 10.5 Hz, 1H), 6.05 (dt, J = 19.9, 9.9 Hz, 3H), 5.64 (dd, J = 10.4, 2.4 Hz, 1H), 4.39 (d, J = 12.7 Hz, 1H), 4.19-4.11 (m, 2H), 4.06 (d, J = 7.2 Hz, 2H), 4.01 (d, J = 5.6 Hz, 1H), 3.72-3.66 (m, 2H), 3.33 (s, 3H), 2.98 (t, J = 12.5 Hz, 1H), 2.59 (t, J = 11.9 Hz, 1H), 2.22-2.10 (m, 1H), 1.53 (s, 2H), 1.18-1.06 (m, 2H). ^{13}C

NMR (101 MHz, DMSO-d_6): δ 164.63, 157.95, 157.74, 152.01, 150.76, 130.12, 129.03, 127.48, 127.38, 123.90, 115.42, 115.11, 100.44, 70.88, 67.45, 58.66, 49.28, 45.22, 41.62, 36.86, 30.70, 29.62. MS (ESI), m/z: 436.22 $[M + H]^+$.

1-(4-((4-Amino-5-(benzo[*d*][1,3]dioxol-5-yl)-7*H*-pyrrolo[2,3-*d*]pyrimidin-7-yl)methyl)piperidin-1-yl)prop-2-en-1-one (B16). Purity: HPLC 96.5%. ^{1}H NMR (400 MHz, DMSO-d_6): δ 8.12 (s, 1H), 7.26 (s, 1H), 7.00 (dd, J = 6.9, 4.8 Hz, 2H), 6.90 (dd, J = 7.9, 1.7 Hz, 1H), 6.77 (dd, J = 16.7, 10.5 Hz, 1H), 6.25-5.95 (m, 5H), 5.65 (d, J = 2.4 Hz, 1H), 4.38 (d, J = 12.7 Hz, 1H), 4.05 (d, J = 7.2 Hz, 2H), 4.01 (s, 1H), 2.98 (s, 1H), 2.57 (d, J = 12.9 Hz, 1H), 2.16 (dd, J = 7.4, 3.5 Hz, 1H), 1.54 (d, J = 12.2 Hz, 2H), 1.14 (d, J = 23.7 Hz, 2H). ^{13}C NMR (101 MHz, DMSO-d_6): δ 164.61, 157.69, 152.04, 150.73, 148.18, 146.72, 129.02, 128.97, 127.40, 124.18, 122.20, 115.25, 109.43, 109.15, 101.56, 100.32, 49.29, 45.21, 41.61, 36.84, 30.70, 29.61. MS (ESI), m/z: 406.22$[M + H]^+$.

1-(4-((4-Amino-5-(4-(hydroxymethyl)phenyl)-7*H*-pyrrolo[2,3-*d*]pyrimidin-7-yl)methyl)piperidin-1-yl)prop-2-en-1-one (B17). Purity: HPLC 97.6%. ^{1}H NMR (400 MHz, DMSO-d_6): δ 8.15 (s, 1H), 7.42 (s, 3H), 7.32 (s, 1H), 6.77 (dd, J = 16.7, 10.5 Hz, 1H), 6.06 (dd, J = 16.7, 2.4 Hz, 3H), 5.64 (dd, J = 10.5, 2.4 Hz, 1H), 4.39 (d, J = 12.5 Hz, 1H), 4.08 (d, J = 7.2 Hz, 2H), 4.03 (dd, J = 14.1, 7.0 Hz, 1H), 2.99 (t, J = 12.4 Hz, 1H), 2.59(t, J = 12.4 Hz, 1H), 2.22-2.11 (m, 1H), 1.55 (d, J = 13.1 Hz, 2H), 1.14 (d, J = 11.6 Hz, 2H). ^{13}C NMR (101 MHz, DMSO-d_6): δ 164.62, 157.69, 152.05, 150.89, 141.44, 133.53, 129.02, 128.63, 127.56, 127.41, 124.33, 115.41, 100.31, 63.13, 49.33, 45.21, 41.62, 36.87, 30.70, 29.61. MS (ESI), m/z: 392.08 $[M + H]^+$.

1-(4-((4-Amino-5-(2,3-dihydrobenzo[*b*][1,4]dioxin-6-yl)-7*H*-pyrrolo[2,3-*d*]pyrimidin-7-yl)methyl)piperidin-1-yl)prop-2-en-1-one (B18). Purity: HPLC 96.3%. ^{1}H NMR (400 MHz, DMSO-d_6): δ 8.12 (s, 1H), 7.24 (s, 1H), 7.00 – 6.86 (m, 3H), 6.77 (dd, J = 16.7, 10.6 Hz, 1H), 6.06 (dd, J = 23.5, 8.5 Hz, 3H), 5.64 (dd, J = 10.4, 2.3 Hz, 1H), 4.38 (d, J = 12.0 Hz, 1H), 4.31-4.23 (m, 4H), 4.05 (d, J = 7.3 Hz, 2H), 4.01 (d, J = 7.1 Hz, 1H), 2.98 (t, J = 12.8 Hz, 1H), 2.58 (t, J = 12.2 Hz, 1H), 2.20-2.09 (m, 1H), 1.52 (s, 2H), 1.13 (d, J = 10.5 Hz, 2H). ^{13}C NMR (101 MHz, DMSO-d_6): δ 164.63,

157.69, 152.02, 150.74, 144.06, 142.95, 129.04, 128.31, 127.38, 124.06, 121.79, 118.00, 117.40, 114.99, 100.30, 64.63, 64.56, 49.29, 45.20, 41.61, 36.83, 30.71, 29.60. MS (ESI), m/z: 420.30 $[M + H]^+$.

Methyl-4-(7-((1-acryloylpiperidin-4-yl)methyl)-4-amino-7*H*-pyrrolo[2,3-*d*]pyrimidin-5-yl)benzoate (B19). Purity: HPLC 98.6%. ^{1}H NMR (400 MHz, DMSO-d_6): δ 8.17 (s, 1H), 8.04 (d, *J* = 8.1 Hz, 2H), 7.61 (d, *J* = 8.1 Hz, 2H), 7.50 (s, 1H), 6.77 (dd, *J* = 16.6, 10.5 Hz, 1H), 6.21 (s, 2H), 6.06 (dd, *J* = 16.7, 1.9 Hz, 1H), 5.68-5.60 (m, 1H), 4.39 (d, *J* = 12.0 Hz, 1H), 4.10 (d, *J* = 7.0 Hz, 2H), 4.06-3.98 (m, 1H), 2.98 (t, *J* = 12.2 Hz, 1H), 2.59 (t, *J* = 12.2 Hz, 1H), 2.18 (s, 1H), 1.54 (s, 2H), 1.16 (dd, *J* = 16.0, 8.9 Hz, 2H). ^{13}C NMR (101 MHz, DMSO-d_6): δ 166.66, 164.62, 157.80, 152.30, 151.47, 140.13, 130.32, 129.00, 128.71, 127.66, 127.42, 125.71, 114.64, 99.92, 49.45, 45.20, 41.61, 36.80, 30.69, 29.60. MS (ESI), m/z: 420.12 $[M + H]^+$.

1-(4-((4-Amino-5-(cyclohex-1-en-1-yl)-7*H*-pyrrolo[2,3-*d*]pyrimidin-7-yl)methyl)piperidin-1-yl)prop-2-en-1-one (B20). Purity: HPLC 97.6%. ^{1}H NMR (400 MHz, DMSO-d_6): δ 8. 08 (s, 1H), 7.17 (s, 1H), 6.77 (dd, *J* = 16.3, 10.1 Hz, 1H), 6.37 (s, 2H), 6.06 (dd, *J* = 16.7, 2.3 Hz, 1H), 5.73 (s, 1H), 5.63 (dd, *J* = 10.5, 2.3 Hz, 1H), 4.37 (d, *J* = 12.1 Hz, 1H), 4.02 (d, *J* = 2.7 Hz, 1H), 4.00 (d, *J* = 7.1 Hz, 2H), 2.96 (t, *J* = 12.1 Hz, 1H), 2.57 (t, *J* = 12.3 Hz, 1H), 2.32 (s, 1H), 2.17 (d, *J* = 6.9 Hz, 2H), 2.10 (d, *J* = 3.8 Hz, 1H), 1.68 (dd, *J* = 35.2, 5.3 Hz, 4H), 1.50 (s, 3H), 1.09 (d, *J* = 6.0 Hz, 2H). ^{13}C NMR (101 MHz, DMSO-d_6): δ 164.60, 157.76, 151.87, 150.40, 132.18, 129.00, 125.81, 123.81, 117.60, 99.89, 49.18, 45.18, 41.60, 36.84, 30.69, 30.05, 29.49, 25.53, 23.04, 22.07. MS (ESI), m/z: 366.21 $[M + H]^+$.

1-(4-((4-Amino-5-(quinolin-7-yl)-7*H*-pyrrolo[2,3-*d*]pyrimidin-7-yl)methyl)piperidin-1-yl)prop-2-en-1-one (B21). Purity: HPLC 96.9%. ^{1}H NMR (400 MHz, DMSO-d_6): δ 8.89 (d, *J* = 2.4 Hz, 1H), 8.40 (d, *J* = 8.1 Hz, 1H), 8.18 (s, 1H), 8.09 (d, *J* = 8.9 Hz, 1H), 8.02 (s, 1H), 7.89 (dd, J = 8.6, 1.7 Hz, 1H), 7.56 (dd, *J* = 8.4, 4.2 Hz, 1H), 7.51 (s, 1H), 6.78 (dd, *J* = 16.6, 10.5 Hz, 1H), 6.22 (s, 2H), 6.07 (dd, *J* = 16.7, 2.1 Hz, 1H), 5.64 (dd, *J* = 10.5, 2.2 Hz, 1H), 4.38 (d, *J* = 12.5 Hz, 1H), 4.12 (d, *J* = 7.0 Hz, 2H), 4.04 (d, *J* = 12.9 Hz, 1H), 3.00 (t, *J* = 12.4 Hz, 1H), 2.60 (t, *J* = 12.1 Hz,

1H), 2.23- 2.11 (m, 1H), 1.56 (s, 2H), 1.17 (d, *J* = 7.1 Hz, 2H). ^{13}C NMR (101 MHz, DMSO-d_6): δ 164.63, 157.89, 152.24, 151.29, 150.59, 147.12, 136.42, 133.28, 131.05, 129.91, 129.02, 128.74, 127.43, 126.96, 125.32, 122.32, 114.97, 100.25, 49.44, 45.23, 41.63, 36.88, 30.72, 29.63. MS (ESI), m/z: 413.29 $[M + H]^+$.

1-(4-((4-Amino-5-(benzofuran-2-yl)-7*H*-pyrrolo[2,3-*d*]pyrimidin-7-yl)methyl)piperidin-1-yl)prop-2-en-1-one (B22). Purity: HPLC 97.0%. ^{1}H NMR (400 MHz, DMSO-d_6): δ 8.18 (s, 1H), 7.91 (s, 1H), 7.64 (t, *J* = 6.8 Hz, 2H), 7.28 (p, *J* = 7.0 Hz, 2H), 7.08 (s, 1H), 6.95 (s, 2H), 6.81-6.73 (m, 1H), 6.07 (dd, *J* = 16.7, 2.1 Hz, 1H), 5.64 (dd, *J* = 10.5, 2.2 Hz, 1H), 4.39 (d, *J* = 12.5 Hz, 1H), 4.12 (d, *J* = 7.1 Hz, 2H), 4.03 (d, *J* = 12.9 Hz, 1H), 2.99 (t, *J* = 12.4 Hz, 1H), 2.59 (t, *J* = 12.1 Hz, 1H), 2.24-2.11 (m, 1H), 1.55 (s, 2H), 1.14 (d, *J* = 5.5 Hz, 2H). ^{13}C NMR (101 MHz, DMSO-d_6): δ 164.63, 157.70, 154.15, 152.64, 151.85, 151.30, 129.40, 129.00, 127.44, 126.09, 124.14, 123.88, 120.98, 111.42, 104.66, 101.46, 99.29, 49.62, 45.18, 41.59, 36.75, 30.63, 29.55. MS (ESI), m/z: 402.30 $[M + H]^+$.

1-(4-((4-Amino-5-(3,5-dimethylisoxazol-4-yl)-7*H*-pyrrolo[2,3-*d*]pyrimidin-7-yl)methyl)piperidin-1-yl)prop-2-en-1-one (B23). Purity: HPLC 98.8%. ^{1}H NMR (400 MHz, DMSO-d_6): δ 8.12 (s, 1H), 7.24 (s, 1H), 6.78 (dd, *J* = 16.7, 10.5 Hz, 1H), 6.14 (s, 2H), 6.06 (dd, *J* = 16.7, 2.4 Hz, 1H), 5.64 (dd, *J* = 10.5, 2.4 Hz, 1H), 4.38 (d, *J* = 12.7 Hz, 1H), 4.06 (d, *J* = 7.3 Hz, 2H), 4.01 (s, 1H), 2.99 (t, *J* = 12.2 Hz, 1H), 2.60 (t, *J* = 12.1 Hz, 1H), 2.30 (s, 3H), 2.17 (ddd, *J* = 15.2, 7.5, 3.4 Hz, 1H), 2.11 (s, 3H), 1.53 (d, *J* = 12.2 Hz, 2H), 1.11 (s, 2H). ^{13}C NMR (101 MHz, DMSO-d_6): δ 166.47, 164.62, 159.68, 157.89, 152.23, 150.69, 129.01, 127.41, 125.90, 109.69, 102.04, 101.05, 49.42, 45.18, 41.61, 36.73, 30.65, 29.54, 11.74, 10.62. MS (ESI), m/z: 381.05 $[M + H]^+$.

1-(4-((4-Amino-5-(4-((3,4-difluorobenzyl)oxy)phenyl)-7*H*-pyrrolo[2,3-*d*]pyrimidin-7-yl)methyl)piperidin-1-yl)prop-2-en-1-one (B24). Purity: HPLC 96.8%. ^{1}H NMR (400 MHz, DMSO-d_6): δ 8.13 (s, 1H), 7.66 (dd, *J* = 15.3, 8.5 Hz, 1H), 7.39 (dd, *J* = 8.6, 2.0 Hz, 2H), 7.35 (dd, *J* = 8.7, 6.2 Hz, 1H), 7.25 (d, *J* = 1.7 Hz, 1H), 7.19 – 7.10 (m, 3H), 6.78 (dd, *J* = 16.7, 10.5 Hz, 1H), 6.07 (dd, *J* = 16.7, 2.4 Hz, 3H), 5.64

(dd, *J* = 10.5, 2.4 Hz, 1H), 5.15 (d, *J* = 3.5 Hz, 2H), 4.39 (d, *J* = 13.0 Hz, 1H), 4.06 (d, *J* = 7.1 Hz, 2H), 4.01 (d, *J* = 7.0 Hz, 1H), 2.98 (t, *J* = 12.2 Hz, 1H), 2.59 (t, *J* = 12.1 Hz, 1H), 2.16 (d, *J* = 3.9 Hz, 1H), 1.55 (d, *J* = 11.2 Hz, 2H), 1.12 (s, 2H). ^{13}C NMR (101 MHz, DMSO-d_6): δ 164.62, 157.75, 157.57, 152.03, 150.78, 132.70, 130.15, 129.01, 127.95, 127.04, 123.98, 118.03, 117.26, 115.79, 115.70, 115.03, 112.09, 104.55, 100.41, 68.46, 49.29, 45.21, 41.62, 36.87, 30.72, 29.62. MS (ESI), m/z: 504.28 $[M + H]^+$.

(*R*)-1-(3-((4-Amino-5-(4-phenoxyphenyl)-7*H*-pyrrolo[2,3-*d*]pyrimidin-7-yl)methyl)piperidin-1-yl)prop-2-en-1-one (B25). Purity: HPLC 98.4%. ^{1}H NMR (400 MHz, DMSO-d_6): δ 8.15 (s, 1H), 7.47 (d, *J* = 8.5 Hz, 2H), 7.41 (t, *J* = 7.9 Hz, 2H), 7.34 (s, 1H), 7.16 (t, *J* = 7.4 Hz, 1H), 7.10 (t, *J* = 7.5 Hz, 4H), 6.70 (ddd, *J* = 60.4, 16.3, 10.6 Hz, 1H), 6.14 (s, 2H), 6.04 (d, *J* = 16.7 Hz, 1H), 5.62 (t, *J* = 11.1 Hz, 1H), 4.21 - 4.05 (m, 3H), 3.92 - 3.77 (m, 1H), 3.15 - 2.85 (m, 1H), 2.67 (t, *J* = 11.3 Hz, 1H), 2.07 (d, *J* = 34.2 Hz, 1H), 1.69 (s, 2H), 1.26 (d, *J* = 18.4 Hz, 2H). ^{13}C NMR (101 MHz, DMSO-d_6): δ 164.67, 157.77, 157.20, 155.98, 152.10, 151.02, 130.53, 130.48, 130.38, 129.00, 127.43, 124.22, 123.94, 119.62, 119.13, 115.01, 100.27, 47.19, 46.18, 45.45, 37.00, 28.31, 25.44. MS (ESI), m/z: 454.21$[M + H]^+$.

(*R*)-1-(3-((4-Amino-5-(benzo[*d*][1,3]dioxol-5-yl)-7*H*-pyrrolo[2,3-*d*]pyrimidin-7-yl)methyl)piperidin-1-yl)prop-2-en-1-one (B26). Purity: HPLC 96.7%. ^{1}H NMR (400 MHz, DMSO-d_6): δ 8.12 (s, 1H), 7.29 (s, 1H), 7.00 (dd, *J* = 8.4, 4.8 Hz, 2H), 6.90 (dd, *J* = 7.9, 1.7 Hz, 1H), 6.74 (dd, *J* = 22.2, 9.0 Hz, 1H), 6.04 (d, *J* = 17.3 Hz, 5H), 5.63 (d, *J* = 11.8 Hz, 1H), 4.11 (m, 1H), 4.07 (d, *J* = 7.6 Hz, 2H), 3.90-3.77 (m, 1H), 3.10 (t, *J* = 11.2 Hz, 1H), 2.67 (t, *J* = 11.2 Hz, 1H), 2.03 (d, *J* = 11.8 Hz, 1H), 1.68 (m, 2H), 1.26 (d, *J* = 9.7 Hz, 2H). ^{13}C NMR (101 MHz, DMSO-d_6): δ 164.66, 157.70, 152.06, 150.82, 148.19, 146.74, 128.97, 127.42, 124.08, 122.20, 109.42, 109.62, 101.56, 100.30, 46.14, 46.17, 45.44, 36.99, 28.29, 25.41. MS (ESI), m/z: 406.22$[M + H]^+$.

(*S*)-1-(3-((4-Amino-5-(4-phenoxyphenyl)-7*H*-pyrrolo[2,3-*d*]pyrimidin-7-yl)methyl)piperidin-1-yl)prop-2-en-1-one (B27). Purity: HPLC 98.8%. ^{1}H NMR (400 MHz, DMSO-d_6): δ 8.15 (s, 1H), 7.47 (d, *J* = 8.5 Hz, 2H), 7.41 (t, *J* = 7.8 Hz, 2H), 7.34 (s,

1H), 7.16 (t, *J* = 7.4 Hz, 1H), 7.10 (t, *J* = 7.5 Hz, 4H), 6.81 - 6.57 (m, 1H), 6.14 (s, 2H), 6.04 (d, *J* = 16.6 Hz, 1H), 5.63 (d, *J* = 10.7 Hz, 1H), 4.19 - 4.05 (m, 3H), 3.92 - 3.77 (m, 1H), 3.10 (s, 1H), 2.67 (s, 1H), 2.07 (d, *J* = 35.0 Hz, 1H), 1.69 (s, 2H), 1.28 (s, 2H). ^{13}C NMR (101 MHz, DMSO-d_6): δ 164.67, 157.77, 157.20, 155.98, 152.10, 151.01, 130.53, 130.48, 130.38, 129.00, 127.42, 124.22, 123.94, 119.62, 119.13, 115.01, 100.27, 47.18, 46.19, 45.45, 37.00, 28.32, 25.43. MS (ESI), m/z: 454.21[M + H]$^+$.

(*S*)-1-(3-((4-Amino-5-(benzo[*d*][1,3]dioxol-5-yl)-7*H*-pyrrolo[2,3-*d*]pyrimidin-7-yl) methyl)piperidin-1-yl)prop-2-en-1-one (B28). Purity: HPLC 97.2%. ^{1}H NMR (400 MHz, DMSO-d_6): δ 8.12 (d, *J* = 5.5 Hz, 1H), 7.29 (s, 1H), 7.01 (dt, *J* = 4.7, 3.1 Hz, 2H), 6.91 (dd, *J* = 7.9, 1.7 Hz, 1H), 6.75 (ddd, *J* = 12.2, 9.6, 6.8 Hz, 1H), 6.25-5.91 (m, 5H), 5.62 (t, *J* = 11.6 Hz, 1H), 4.13 (dd, *J* = 8.3, 5.0 Hz, 1H), 4.06 (d, *J* = 7.6 Hz, 2H), 3.84 (dd, *J* = 25.1, 12.9 Hz, 1H), 3.08 (t, *J* = 11.5 Hz, 1H), 2.67 (t, *J* = 11.5 Hz, 1H), 2.13-2.00 (m, 1H), 1.68 (s, 2H), 1.32-1.22 (m, 2H). ^{13}C NMR (101 MHz, DMSO-d_6): δ 164.66, 157.70, 152.06, 150.82, 148.19, 146.74, 128.97, 127.42, 124.08, 122.20, 109.42, 109.62, 101.56, 100.30, 46.15, 46.17, 45.44, 36.99, 28.30, 25.41. MS (ESI), m/z: 406.23 [M + H]$^+$.

1-(4-(2-(4-Amino-5-(4-phenoxyphenyl)-7*H*-pyrrolo[2,3-*d*]pyrimidin-7-yl)ethyl)pi peridin-1-yl)prop-2-en-1-one (B29). Purity: HPLC 98.1%. ^{1}H NMR (400 MHz, DMSO-d_6): δ 8.15 (s, 1H), 7.46 (d, *J* = 8.5 Hz, 2H), 7.41 (dd, *J* = 11.2, 4.2 Hz, 2H), 7.36 (s, 1H), 7.15 (t, *J* = 7.4 Hz, 1H), 7.09 (dd, *J* = 7.8, 6.3 Hz, 4H), 6.78 (dd, *J* = 16.7, 10.5 Hz, 1H), 6.06 (dd, *J* = 16.7, 2.4 Hz, 3H), 5.63 (dd, *J* = 10.4, 1.9 Hz, 1H), 4.37 (d, *J* = 12.6 Hz, 1H), 4.21 (t, *J* = 7.1 Hz, 2H), 4.01 (t, *J* = 10.4 Hz, 1H), 2.96 (t, *J* = 12.6 Hz, 1H), 2.56 (t, *J* = 12.1 Hz, 1H), 1.75 (dd, *J* = 13.4, 6.6 Hz, 4H), 1.47 (s, 1H), 1.11 - 0.98 (m, 2H). ^{13}C NMR (101 MHz, DMSO-d_6): δ 164.54, 157.73, 157.20, 155.93, 152.02, 150.69, 130.53, 130.47, 129.08, 127.26, 123.94, 123.62, 119.60, 119.12, 115.07, 100.31, 45.60, 41.99 41.69, 36.62, 33.34, 32.81, 31.78. MS (ESI), m/z: 468.23[M + H]$^+$.

1-(4-(2-(4-Amino-5-(benzo[*d*][1,3]dioxol-5-yl)-7*H*-pyrrolo[2,3-*d*]pyrimidin-7-yl)et

hyl)piperidin-1-yl)prop-2-en-1-one (B30). Purity: HPLC 97.9%. ^{1}H NMR (400 MHz, DMSO-d_6): δ 8.13 (s, 1H), 7.31 (s, 1H), 7.00 (t, J = 4.7 Hz, 2H), 6.90 (dd, J = 7.9, 1.7 Hz, 1H), 6.82 - 6.74 (m, 1H), 6.23 - 5.98 (m, 5H), 5.63 (dd, J = 10.3, 1.7 Hz, 1H), 4.37 (d, J = 12.4 Hz, 1H), 4.18 (t, J = 7.0 Hz, 2H), 4.01 (dd, J = 14.4, 7.7 Hz, 1H), 2.96 (t, J = 12.4 Hz, 1H), 2.56 (t, J = 12.2 Hz, 1H), 1.83 - 1.69 (m, 4H), 1.47 (s, 1H), 1.10 - 0.98 (m, 2H). ^{13}C NMR (101 MHz, DMSO-d_6): δ 164.54, 157.66, 151.99, 150.49, 148.17, 146.69, 129.08, 129.06, 127.25, 123.47, 122.18, 115.48, 109.43, 109.14, 101.55, 100.34, 45.60, 41.98, 41.65, 36.61, 33.33, 32.81, 31.77. MS (ESI), m/z: 420.19[M + H]$^{+}$.

5-(4-Phenoxyphenyl)-7-((1-(vinylsulfonyl)piperidin-4-yl)methyl)-7*H*-pyrrolo[2,3-*d*]pyrimidin-4-amine (B31). Purity: HPLC 97.9%. ^{1}H NMR (400 MHz, DMSO-d_6) : δ 8.13 (s, 1H), 7.31 (s, 1H), 7.00 (dd, J = 7.5, 4.8 Hz, 2H), 6.93-6.87 (m, 2H), 6.10 (dd, J = 13.9, 12.7 Hz, 6H), 4.17 (dd, J = 7.2, 2.4 Hz, 2H), 3.35-3.29 (m, 1H), 3.24 (dd, J = 10.2, 7.3 Hz, 1H), 3.20-3.14 (m, 1H), 3.02 (dd, J = 10.1, 7.0 Hz, 1H), 2.78 (dt, J = 14.3, 7.2 Hz, 1H), 1.92-1.84 (m, 1H), 1.64 (dd, J = 12.5, 7.8 Hz, 1H). ^{13}C NMR (101 MHz, DMSO-d_6): δ 157.81, 157.19, 156.05, 152.13, 150.86, 130.58, 130.53, 130.23, 123.95, 121.03, 119.60, 119.57, 119.12, 115.78, 100.64, 60.23, 49.07, 45.46, 35.95, 29.22, 21.19. MS (ESI), m/z: 428.19 [M + H]$^{+}$.

(*E*)-1-(4-((4-Amino-5-(4-phenoxyphenyl)-7*H*-pyrrolo[2,3-*d*]pyrimidin-7-yl)methyl)piperidin-1-yl)-4-(dimethylamino)but-2-en-1-one (B32). Purity: HPLC 97.1%. ^{1}H NMR (400 MHz, DMSO-d_6): δ 8.14 (s, 1H), 7.50-7.39 (m, 5H), 7.31 (s, 1H), 7.16 (t, J = 7.4 Hz, 1H), 7.13-7.07 (m, 4H), 6.58 (d, J = 6.3 Hz, 1H), 6.12 (s, 2H), 4.38 (d, J = 11.6 Hz, 1H), 4.07 (d, J = 7.2 Hz, 2H), 4.01 (d, J = 12.7 Hz, 1H), 3.09 (d, J = 5.0 Hz, 2H), 2.98 (t, J = 12.4 Hz, 1H), 2.57 (t, J = 12.4 Hz, 1H), 2.20 (s, 6H), 1.55 (d, J = 12.0 Hz, 2H), 1.18-1.05 (m, 2H). ^{13}C NMR (101 MHz, DMSO-d_6): δ 164.00, 157.81, 157.19, 156.05, 152.13, 150.86, 141.98, 130.58, 130.53, 130.23, 123.95, 121.03, 119.60, 119.57, 119.12, 115.78, 100.64, 60.28, 60.23, 53.43, 50.97, 45.50, 45.46, 44.49, 31.58, 29.79. MS (ESI), m/z: 511.41 [M + H]$^{+}$.

5-(Benzo[*d*][1,3]dioxol-5-yl)-7-((1-(vinylsulfonyl)piperidin-4-yl)methyl)-7*H*-pyrro

lo[2,3-*d*]pyrimidin-4-amine (B33). Purity: HPLC 97.8%. ^{1}H NMR (400 MHz, DMSO-d_6): δ 8.12 (s, 1H), 7.26 (s, 1H), 7.01 (d, J = 8.8 Hz, 2H), 6.94-6.86 (m, 1H), 6.75 (dd, J = 16.5, 10.0 Hz, 1H), 6.26-6.01 (m, 6H), 4.07 (d, J = 7.2 Hz, 2H), 3.51 (d, J = 12.0 Hz, 2H), 2.57 (t, J = 11.3 Hz, 2H), 1.99 (s, 1H), 1.60 (d, J = 12.0 Hz, 2H), 1.35-1.21 (m, 2H). ^{13}C NMR (101 MHz, DMSO-d_6): δ 157.69, 152.05, 150.73, 148.19, 146.73, 133.65, 129.09, 128.94, 124.13, 122.19, 115.31, 109.43, 109.15, 101.56, 100.31, 60.22, 49.09, 45.43, 35.95, 29.21, 21.23. MS (ESI), m/z: 442.23 $[M + H]^+$.

(*E*)-1-(4-((4-Amino-5-(benzo[*d*][1,3]dioxol-5-yl)-7*H*-pyrrolo[2,3-*d*]pyrimidin-7-yl) methyl)piperidin-1-yl)-4-(dimethylamino)but-2-en-1-one (B34). Purity: HPLC 98.3%. ^{1}H NMR (400 MHz, DMSO-d_6): δ 8.12 (s, 1H), 7.26 (s, 1H), 7.03-6.98 (m, 2H), 6.90 (d, J = 7.9 Hz, 1H), 6.60-6.54 (m, 2H), 6.06 (s, 4H), 4.38 (d, J = 12.5 Hz, 1H), 4.05 (d, J = 7.1 Hz, 2H), 3.99 (s, 1H), 3.00 (d, J = 3.0 Hz, 2H), 2.97 (t, J = 12.4 Hz, 1H), 2.54 (t, J = 12.4 Hz, 1H), 2.13 (s, 6H), 2.11 (s, 1H), 1.54 (d, J = 11.2 Hz, 2H), 1.11 (s, 2H). ^{13}C NMR (101 MHz, DMSO-d_6): δ 164.22, 157.68, 152.30, 150.72, 148.18, 146.72, 139.61, 128.96, 124.69, 124.20, 122.20, 115.26, 109.42, 109.15, 101.57, 100.32, 59.62, 49.29, 45.28, 44.67, 41.62, 36.87, 30.69, 29.62. MS (ESI), m/z: 463.14 $[M + H]^+$.

1-(4-((4-Amino-3-(4-phenoxyphenyl)-1*H*-pyrazolo[3,4-*d*]pyrimidin-1-yl)methyl)p iperidin-1-yl)prop-2-en-1-one (B35). Purity: HPLC 96.0%. ^{1}H NMR (400 MHz, DMSO-d_6): δ 8.25 (s, 1H), 7.67 (d, J = 8.6 Hz, 2H), 7.44 (t, J = 7.8 Hz, 2H), 7.22 - 7.10 (m, 5H), 6.77 (dd, J = 16.7, 10.5 Hz, 1H), 6.06 (dd, J = 16.7, 2.3 Hz, 1H), 5.76 (s, 2H), 5.63 (dd, J = 10.5, 2.1 Hz, 1H), 4.38 (d, J = 12.3 Hz, 1H), 4.25 (d, J = 7.0 Hz, 2H), 4.08 – 3.94 (m, 1H), 2.99 (t, J = 12.0 Hz, 1H), 2.60 (t, J = 12.2 Hz, 1H), 2.28 - 2.14 (m, 1H), 1.57 (d, J = 12.1 Hz, 2H), 1.18 - 1.05 (m, 2H). ^{13}C NMR (101 MHz, DMSO-d_6): δ 164.64, 158.67, 157.56, 156.23, 155.05, 143.60, 130.61, 130.52, 129.05, 128.43, 127.35, 124.27, 119.46, 97.55, 51.63, 45.18, 41.55, 36.71, 30.71, 29.61. MS (ESI), m/z: 455.25 $[M + H]^+$.

3-(4-Phenoxyphenyl)-1-((1-(vinylsulfonyl)piperidin-4-yl)methyl)-1*H*-pyrazolo[3,4

-*d*]pyrimidin-4-amine (B36). Purity: HPLC 97.1%. ^{1}H NMR (400 MHz, DMSO-d_6): δ 8.25 (s, 1H), 7.66 (d, J = 8.6 Hz, 2H), 7.44 (t, J = 7.9 Hz, 2H), 7. 19 (t, J = 8.6 Hz, 1H), 7.14 (dd, J = 10.4, 8.6 Hz, 4H), 6.75 (dd, J = 16.5, 10.0 Hz, 1H), 6.09 (dd, J = 17.4, 13.3 Hz, 2H), 4.27 (d, J = 6.9 Hz, 2H), 3.51 (d, J = 12.1 Hz, 2H), 2.59 (t, J = 11.1 Hz, 2H), 2.08 (d, J = 3.3 Hz, 1H), 1.62 (d, J = 11.4 Hz, 2H), 1.37 - 1.25 (m, 2H). ^{13}C NMR (101 MHz, DMSO-d_6): δ 158.67, 157.58, 156.25, 156.25, 155.06, 143.64, 133.74, 130.61, 130.53, 129.04, 128.40, 124.28, 119.46, 119.44, 97.57, 51.41, 45.42, 35.82, 29.19. MS (ESI), m/z: 498.40 $[M + H]^+$.

1-(4-((4-Amino-3-(benzo[*d*][1,3]dioxol-5-yl)-1*H*-pyrazolo[3,4-*d*]pyrimidin-1-yl)methyl)piperidin-1-yl)prop-2-en-1-one (B37). Purity: HPLC 97.8%. ^{1}H NMR (400 MHz, DMSO-d_6): δ 8.22 (s, 1H), 7.17 - 7.10 (m, 2H), 7.07 (d, J = 7.9 Hz, 1H), 6.80 - 6.71 (m, 1H), 6.11 (s, 2H), 6.06 (dd, J = 16.7, 2.4 Hz, 1H), 5.63 (dd, J = 10.5, 2.4 Hz, 1H), 4.37 (d, J = 13.0 Hz, 1H), 4.23 (d, J = 7.0 Hz, 2H), 4.03 (d, J = 7.0 Hz, 1H), 2.99 (t, J = 12.5 Hz, 1H), 2.60 (t, J = 12.0 Hz, 1H), 2.22 (ddd, J = 17.6, 8.8, 5.3 Hz, 1H), 1.57 (d, J = 12.6 Hz, 2H), 1.15 (dd, J = 16.0, 9.8 Hz, 2H). ^{13}C NMR (101 MHz, DMSO-d_6): δ 164.63, 158.62, 156.21, 154.92, 148.34, 148.21, 143.88, 129.06, 127.34, 127.19, 122.71, 109.34, 109.00, 101.84, 97.52, 51.58, 45.17, 41.59, 36.70, 30.71, 29.61. MS (ESI), m/z: 407.23 $[M + H]^+$.

3-(Benzo[*d*][1,3]dioxol-5-yl)-1-((1-(vinylsulfonyl)piperidin-4-yl)methyl)-1*H*-pyrazolo[3,4-*d*]pyrimidin-4-amine (B38). Purity: HPLC 96.9%. ^{1}H NMR (400 MHz, DMSO-d_6): δ 8.23 (s, 1H), 7.17 - 7.10 (m, 2H), 7.07 (d, J = 7.9 Hz, 1H), 6.75 (dd, J = 16.5, 10.0 Hz, 1H), 6.09 (dd, J = 18.6, 12.2 Hz, 4H), 4.24 (d, J = 6.9 Hz, 2H), 3.50 (d, J = 12.2 Hz, 2H), 2.59 (dd, J = 11.9, 10.1 Hz, 2H), 2.12 - 2.00 (m, 1H), 1.62 (d, J = 11.4 Hz, 2H), 1.35 - 1.25 (m, 2H). ^{13}C NMR (101 MHz, DMSO-d_6): δ 158.62, 156.22, 154.92, 148.34, 148.21, 143.92, 133.74, 129.03, 127.16, 122.72, 109.34, 109.01, 101.84, 97.54, 51.37, 45.42, 35.81, 29.19. MS (ESI), m/z: 443.34 $[M + H]^+$.

Enzymatic Assay. The enzymatic activities of all synthesized compounds against Btk were assessed using the Caliper Mobility Shift Assay in the presence of K_m ATP (ChemPartner; Shanghai; China). The assay protocol guide is commercially available

from ChemPartner. The activities against other kinases were tested by EurofinsCerep (CEREP, Celle l'Evescault, France). The protocols are available from http://www.cerep.fr/Cerep/Users/index.asp. The assay protocol guide can be accessed at www.eurofins.com/discovery.

Cytotoxicity assay. Cells were plated in 96 well plates containing 100 μL of culture medium. Compounds with indicated concentrations were added to wells and incubated for 72 h. MTT was subsequently added for an extra 2-3 h of incubation. The MTT formazan precipitate was dissolved in DMSO, and the absorbance was measured at a wavelength of 570 nm by a Spectramax M5 microtiter plate luminometer (Molecular Devices, Sunnyvale, CA, USA). IC_{50} values were calculated from dose-response curves obtained from at least three independent experiments.

hERG Activities assay. A CHO cell line stably transfected with hERG cDNA and expressing hERG channels of P25 was used for the study. Cells were maintained in petri dishes or flasks at 37 °C in a humidified incubator with 5% CO_2 and cultured in medium containing Ham's F12, 10% (v/v) heat inactivated FBS, 100 μg/mL Hygromycin B and 100 μg/mL Geneticin. Cells were allowed to grow and reach a confluence rate at about 80-90% in the above condition. Before the experiment, the cells were treated with Detachin (from Genlantis) for 3-5 min. at 37 °C followed by gentle pipette titration 15-20 times at r.t. with culture media, then the cells were re-suspended in serum-free culture medium containing CHO-S-SFM II medium(from Invitrogen) buffered with HEPES (25 mM). The cells used in QPatch study must meet following criteria: under microscopy examination, the majority of cells in suspension should be single and isolated; their viability should be greater than 95%, with only a few debris and cell clumps (which may clog the holes in QPlate during whole-cell clamp recording); cell density should be ranged within 3-8 × 10_6 cells / mL in the final suspension before applying to the QPatch stir chamber. Cells in such condition can be used for recording only for four hours after harvesting. **B16** was finally made into six doses (0.4, 1.2, 3.7, 11.1, 33.3 and 100 μM) DMSO stock, while the doses of positive control cisapride were 3, 1, 0.3, 0.1, 0.03, and 0.01 μM. The cells recordings were

performed using automated QPatch (Sophion Biosciences, Denmark) at r.t.. Data were analyzed using Assay Software provided by Sophion (assay software V5.0), Microsoft Excel and Graphpad Prism 5.0.

Single dose toxicity test. Six male and six female BALB/c mice were oral administration **B16** at a dose of 2.0 g/kg. The general conditions (activity, energy, hair, feces, behavior pattern and other clinical signs), body weight, and mortality of mice were observed carefully. Mice were sacrificed at the end of 7th day, their major organs including heart, liver, spleen, lung and kidney were removed and fixed in 4% paraformaldehyde, and stained with H&E for further histopathological examination.

Kinetics study. 1) A series of conversion data of enzyme were tested after incubated with inhibitor. Based on the IC_{50} (21.7 nM) of compound B16 to inhibit Btk, the tested concentrations of B16 were set as 0 nM, 8 nM, 12 nM, 18 nM, 26 nM, 40 nM, 59 nM, 89 nM, 133 nM, 200 nM. Thus, a series of conversions % were collected after Btk was incubated with corresponding concentrations of B16. 2) K_{on} calculation. Fit the conversion and compound concentration in Graph Pad Prism 5 to get Kobs with the equation Y = (Vi/Kobs)(1-exp(-Kobs*x))+c; Y is conversion; x is compound concentration; Vi is the slope of max control (reaction with enzyme and without compound). Fit the data in Graph Pad Prism 5 to obtain K_{on} value with the equation Y = k3*x + k4; Y is Kobs; X is compound concentration and k3 is K_{on} value.

Western Blotting. Daudi, U2932 and Raji cells were rested for 1 to 24 h at 1 × 10^6 cells/mL in RPMI-1640 (Gibco) with 10% fetal bovine serum (FBS). 1 × 10^6 cells in serum-free RPMI-1640 were pre-incubated with DMSO, serially diluted compound **B16**, for 1 h. Then the cells were stimulated with 10 μg/mL anti-human IgM F(ab')2 (Jackson Immuno Research Laboratories) for the times indicated. Cells were washed in 1×PBS buffer and lysed in cell lysis buffer at 4 °C for 30 min. The lysates were cleared by centrifugation, and the protein concentrations were measured by BCA analysis (Beyotime, China). Lysates containing 50 mg of total proteins were fractionated on a 10% SDS polyacrylamide gel (Bio-Rad) and transferred to Hybond-P PVDF Membrane (Millipore). Incubation of primary antibodies was

performed overnight at 4 °C using 1:1000 Btk, Phospho-Btk (Tyr223), Phospho-Btk (Tyr551), PLCγ2, Phospho-PLCγ2 (Tyr1217) antibody (Abcam). Anti-rabbit (Abcam) horseradish peroxidase-conjugated secondary antibodies and Super Signal West Pico Chemiluminescent Substrate (Thermo) were used to develop the blots.

Pharmacokinetics in Sprague-Dawley rats. Two groups (n = 5) of male and female Sprague-Dawley rats were fasted overnight and received **B16** as an intravenous dose (3 mg/kg) or by oral gavage (3 mg/kg). Blood samples (0.4 mL)were obtained from jugular vein bleeding at 5 min, 15 min, 30 min, 1 h, 2 h, 4 h, 6 h, 8 h, 10 h, 12 h, and 24 h post dose for the p.o. group. At each time point, three mice were bled resulting in a composite pharmacokinetic profile. The tubes were inverted several times to ensure mixing and placed on ice. The blood samples were centrifuged to obtain the plasma fraction. The plasma samples were deproteinized with acetonitrile containing an internal standard. After centrifugation, the supernatant was diluted and centrifuged again. The compound concentrations in the supernatant were measured by a high performance liquid chromatography-tandem mass spectrometry (LC/MS/MS), and the C_{max} is the average of maximum compound concentration of 5 rats in each group. The T_{max} is the average of the time with C_{max} of 5 rats in each group. Other obtained pharmacokinetic parameters are processed by the software DAS 2.0 through inputting each time point and its corresponding compound's concentration.

Metabolic stability in liver microsomes. Compound **B16** (100 μM/L) was incubated with liver microsomes of different species (including human, dog, rat, mice and monkey) in a reaction mixture containing 0.1 M PBS (pH 7.4) and NADPH regeneration system, at 37 °C, in a total reaction volume of 100 μL. Reactions were terminated at 0, 5, 15, 30, 45, 60 and 90 min of incubation with a chilled mixture of acetonitrile. The mixture was vortexed for 3 min, centrifuged at 13000 rpm for 10 min, and the supernatants were analyzed by LC-MS/MS. Stability was assessed by plotting the percent of parent compound remaining against time on a log-linear scale, and half-life was estimated from the linear portion of the log-linear curve using the first order equation $t_{1/2} = 0.693/k$, where k is the slope of the curve (equal to the first order

elimination rate constant). The clearance rate was calculated by the equation Cl_{int} = 0.693/ $t_{1/2}$.

Metabolism-dependent CYP inhibition assay. The experiment of testing **B16**'s inhibitory activity to cytochrome P450 was conducted according to the procedure of metabolism-dependent CYP inhibition assay in reference 34. Phenacetin, tolbutamide, omeprazole and chlorzoxazone were respectively selected as substrates for CYP1A2, 2C9, 2C19, 2D4 and 2E1, and dextromethorphan was the substrate for CYP3A4 and 2D6.

Covalent docking: The Crystal structure of the Btk kinase domain was obtained from the Protein Data Bank (PDB code 5P9J) [31]. 3D structures of the selected compounds were generated and optimized by the Discovery Studio 3.1 package (Accelrys, San Diego, CA, USA). Compounds were docked into the Btk kinase domain using the program Covalent Dock Clound (http://docking.sce.ntu.edu.sg), which was used to perform the covalent docking simulations [32]. Figures were generated though the Professional graphics software Pymol 1.7.

Collagen-Induced Arthritis Model in the Mice. The collagen-induced arthritis (CIA) model shares a number of pathologic, genetic, and immunologic features with RA. Therefore, the CIA mouse model was used to evaluate the effects of oral **B16** (20 mg/kg p.o.) on joint inflammation and histopathology. Arthritis was induced in 10-weekend male DBA/1J mice by immunizations with a 1:1 emulsion of bovine type II collagen (Chondrex) and Freund's complete adjuvant (Sigma-Aldrich) on day 0 and a 1:1 emulsion of bovine type II collagen in Freund's incomplete adjuvant (Sigma-Aldrich). Treatment was initiated when > 20% of mice demonstrated signs of disease. On the day treatment was initiated, the mice were randomly assigned to controls (no collagen injection plus vehicle; n = 8), collagen plus vehicle (n = 8), collagen plus **B16** 20 mg/kg (n = 8) and collagen plus ibrutinib 20 mg/kg (n = 8). Mice were scored for signs of arthritis daily for 30 days. CIA development was inspected three times per week and inflammation of the four paws was graded from 0 to 4 (grade 0, paws with no swelling and focal redness; grade 1, paws with swelling of

finger joints; grade 2, paws with mild swelling of ankle or wrist joints; grade 3, paws with severe inflammation of the entire paw; and grade 4, paws with deformity or ankylosis). Each paw was graded and the four scores were totaled so that the possible maximum score per mouse was 16.

Associated content

Supporting Information: The weight changes in CIA mice with treatment of ibrutinib and **B16** (**Figure S1**). H&E staining of major organs (heart, liver, spleen, lung and kidneys) after oral administration **B16** at a dosage of 2.0 g/kg on day 7 (**Figure S2**). ^{1}H-NMR and ^{13}C-NMR spectra for all final new compounds (**Figure S3-S74**).

Author Information

Corresponding Author

Phone: +86-28-85164063. Fax: +86-28-85164060. E-mail: chenlijuan125@163.com (L-J. Chen.)

Acknowledgment

Authors greatly appreciate the financial support from National Natural Science Foundation of China (81673289) and Guangdong Innovative Research Team Program (Grant 2011Y073).

References

[1] R.W. Hendriks. Drug discovery: New Btk inhibitor holds promise. Nat Chem Biol. 7 (2011) 4-5.

[2] Z. Pan. Bruton's tyrosine kinase as a drug discovery target. Drug News Perspect. 21 (2008) 357-362.

[3] A. Hamasy, Q. Wang, K.E. Blomberg, D.K. Mohammad, L. Yu, et al. Substitution scanning identifies a novel, catalytically active ibrutinib-resistant BTK cysteine 481

to threonine (C481T) variant. Leukemia. 31 (2017) 177-185.

[4] B. Wang, Y. Deng, Y. Chen, K. Yu, A. Wang, et al. Structure-activity relationship investigation for benzonaphthyridinone derivatives as novel potent Bruton's tyrosine kinase (BTK) irreversible inhibitors. Eur. J. Med. Chem. 137 (2017) 545-557.

[5] G.V. De Lucca, Q. Shi, Q. Liu, D.G. Batt, M. Beaudoin Bertrand, et al. Small Molecule Reversible Inhibitors of Bruton's Tyrosine Kinase (BTK): Structure-Activity Relationships Leading to the Identification of 7-(2-Hydroxypropan-2-yl)-4-[2-methyl-3-(4-oxo-3,4-dihydroquinazolin-3-yl)phenyl]-9H-carbazole-1-carboxamide (BMS-935177). J Med Chem. 59 (2016) 7915-7935.

[6] S.H. Watterson, G.V. De Lucca, Q. Shi, C.M. Langevine, et al. Discovery of 6-Fluoro-5-(R)-(3-(S)-(8-fluoro-1-methyl-2,4-dioxo-1,2-dihydroquinazolin-3(4H)-yl)-2-methylphenyl)-2-(S)-(2-hydroxypropan-2-yl)-2,3,4,9-tetrahydro-1H-carbazole-8-carboxamide (BMS-986142): A Reversible Inhibitor of Bruton's Tyrosine Kinase (BTK) Conformationally Constrained by Two Locked Atropisomers. J Med Chem. 9 (2016) 9173-9200.

[7] I.B. McInnes, G. Schett. The pathogenesis of rheumatoid arthritis. N Engl J Med. 365 (2011) 2205-2219.

[8] J.S. Smolen, D. Aletaha, I.B. McInnes. Rheumatoid arthritis. The Lancet. 388 (2016) 2023-2038.

[9] J.A. Whang, B.Y. Chang. Bruton’s tyrosine kinase inhibitors for the treatment of rheumatoid arthritis. Drug Discovery Today. 19 (2014) 1200-1204.

[10] A. Akinleye, Y Chen, N. Mukhi, Y. Song, D. Liu. Ibrutinib and novel BTK inhibitors in clinical development. J Hematol Oncol. 6 (2013) 59.

[11] Y. Lou, X. Han, A. Kuglstatter, R.K. Kondru, Z.K. Sweeney, et al. Structure-based drug design of RN486, a potent and selective Bruton's tyrosine kinase (BTK) inhibitor, for the treatment of rheumatoid arthritis. J Med Chem. 58 (2015) 512-516.

[12] Q. Liang, Y. Chen, K. Yu, C. Chen, S. Zhang, et al. Discovery of N-(3-(5-((3-acrylamido-4-(morpholine-4-carbonyl)phenyl)amino)-1-methyl-6-oxo-1,6

-dihydropyridin-3-yl)-2-methylphenyl)-4-(tert-butyl)benzamide(CHMFL-BTK-01) as a highly selective irreversible Bruton's tyrosine kinase (BTK) inhibitor. Eur. J. Med. Chem. 131 (2017) 107-125.

[13] X. Zhao, M. Xin, Y. Wang, W. Huang, Q. Jin. Discovery of thieno[3,2-c]pyridin-4-amines as novel Bruton's tyrosine kinase (BTK) inhibitors. Bioorg Med Chem. 23 (2015) 6059-6068.

[14] L.A. Honigberg, A.M. Smith, M. Sirisawad, E. Verner, D. Loury, et al. The Bruton tyrosine kinase inhibitor PCI-32765 blocks B-cell activation and is efficacious in models of autoimmune disease and B-cell malignancy. Proc Natl Acad Sci U S A. 107 (2010) 13075-13080.

[15] B.Y. Chang, M.M. Huang, M. Francesco, J. Chen, J. Sokolove, et al. The Bruton tyrosine kinase inhibitor PCI-32765 ameliorates autoimmune arthritis by inhibition of multiple effector cells. Arthritis Res Ther. 13 (2011) R115.

[16] J. Wu, M. Zhang, D. Liu. Acalabrutinib (ACP-196): a selective second generation BTK inhibitor. J Hematol Oncol. 9 (2016) 21.

[17] C. Lee, M.A. Rattu, M.A. Kim. A review of a novel, Bruton’s tyrosine kinase inhibitor, ibrutinib. J Oncol Pharm Practice. 22 (2016) 92-104.

[18] Pharmacology Review: Imbruvica (ibrutinib). FDA.

[19] H.S. Walter, S.A. Rule; M.J. Dyer, L. Karlin, C. Jones, et al. A phase 1 clinical trial of the selective BTK inhibitor ONO/GS-4059 in relapsed and refractory mature B-cell malignancies. Blood. 127 (2016) 411-419.

[20] R.R. Shah, J. Morganroth, D.R. Shah. Update on Cardiovascular Safety of Tyrosine Kinase Inhibitors: With a special focus on QT interval, left ventricular dysfunction and overall risk/benefit. Drug Saf. 36 (2013) 295-316.

[21] F. Shakeel, M. Iqbal, E. Ezzeldin. Bioavailability enhancement and pharmacokinetic profile of an anticancer drug ibrutinib by self-nanoemulsifying drug delivery system. J Pharm Pharmacol. 68 (2016) 772-780.

[22] F. Shakeel, M.M. Salem-Bekhit, M. Iqbal, N. Haq. Solubility and thermodynamic function of a new anticancer drug ibrutinib in 2-(2-ethoxyethoxy)ethanol + water

mixtures at differen temperatures. J. Chem. Thermodynamics. 89 (2015) 159-163.

[23] M. Xin, X. Zhao, W. Huang, Q. Jin, G. Wu, et al. Synthesis and biological evaluation of novel 7-substituted 3-(4-phenoxyphenyl)thieno[3,2-c]pyridin-4-ami- nes as potent Bruton's tyrosine kinase (BTK) inhibitors. Bioorg Med Chem. 23 (2015) 6250-6257.

[24] S.E. Lazerwith, G. Bahador, E. Canales, C. Cheng, L. Chong, et al. Optimization of Pharmacokinetics through Manipulation of Physicochemical Properties in a Series of HCV Inhibitors. ACS Med Chem Lett. 2 (2011)715-719.

[25] N.B. Ramsey, O.S. Andersen. Bilayer Effects of Antimalarial Compounds. PLoS One. 10 (2015) e0142401.

[26] O.S. Smith, D.R. Dougan, M. Komandla, T. Kanouni, B. Knight, et al. Fragment-Based Discovery of a Small Molecule Inhibitor of Bruton’s Tyrosine Kinase. J. Med. Chem. 58 (2015) 5437-5444.

[27] A.T. Miller, L.J. Berg. New insights into the regulation and functions of Tec family tyrosine kinases in the immune system. Curr Opin Immunol. 14 (2002) 331-340.

[28] J. Gomez-Rodriguez, J.A. Readinger, I.C. Viorritto. et al. Tec kinases, actin, and cell adhesion. Immunol Rev. 218 (2007) 45-64.

[29] F. De Ponti, E. Poluzzi, N. Montanaro. QT-interval prolongation by non-cardiac drugs: lessons to be learned from recent experience. Eur J Clin Pharmacol. 56 (2000) 1-18.

[30] J. Tamargo. Drug-induced torsade de pointes: from molecular biology to bedside. Jpn J Pharmacol. 83 (2000) 1-19.

[31] A.T. Bender, A. Gardberg, A. Pereira, et al. The ability of Btk inhibitors to sequester Y551 and prevent phosphorylation determines potency for inhibition of FcR but not B cell receptor signaling. Mol Pharmacol. 91 (2017) 208-219.

[32] X. Ouyang, S. Zhou, C.T.T. Su, Z. Ge, R. Li, C.K. Kwoh, Covalent Dock: Automated covalent docking with parameterized covalent linkage energy estimation and molecular geometry constrains. J. Comput. Chem. 34 (2013) 326-336.

[33] S. Sharma, J. Singh, R. Ojha, H. Singh, M. Kaur, et al. Design strategies, structure activity relationship and mechanistic insights for purines as kinase inhibitors. Eur. J. Med. Chem. 112 (2016) 298-346.

[34] J.S. Jeon, S.J. Oh, J. Lee, C.S. Ryu, Y. Kim, B.H. Lee, S.K. Kim. Metabolic characterization of *meso*-dihydroguaiaretic acid in liver microsomes and in mice. Food Chem. Toxicol. 76 (2015) 94-102.

Highlights

- A series of novel compounds bearing 7*H*-pyrrolo[2,3-*d*]pyrimidin-4-amine scaffold have been synthesized and identified as potent Btk inhibitors.
- Compound **B16** significantly inhibited Btk (IC_{50} = 21.70 ± 0.82nM) with moderate kinase selectivity.
- **B16** showed weaker inhibition to hERG channel (IC_{50} = 11.10μM) than ibrutinib (IC_{50} = 0.97μM).
- Owing to its favorable physicochemical properties (ClogP = 2.53, aqueous solubility ≈ 0.1mg/ml) and pharmacokinetic profiles (F = 49.15%, $t_{1/2}$ = 7.02h), **B16** exhibited slightly better anti-arthritis efficacy than ibrutinib in CIA mice.